Evaluation of Modal Pushover-based Scaling of one Component of Ground Motion: Tall Buildings

Erol Kalkan & Anil K. Chopra

Corresponding author: Dr. Erol Kalkan, P.E.

Mailing address: United States Geological Survey
Earthquake Science Center
MS977, 345 Middlefield Rd.
Menlo Park, CA, 94025

Phone: (650) 329-5146
E-mail: ekalkan@usgs.gov

Keywords: Ground motion scaling, tall building, nonlinear response history analysis, seismic design; higher-mode effects; inelastic response; performance-based engineering

Evaluation of Modal Pushover-based Scaling of one Component of Ground Motion: Tall Buildings

Erol Kalkan, [a] M.EERI, and Anil K. Chopra [b] M.EERI

Nonlinear response history analysis (RHA) is now increasingly used for performance-based seismic design of tall buildings. Required for nonlinear RHAs is a set of ground motions selected and scaled appropriately so that analyses results would be *accurate* (unbiased) and *efficient* (having relatively small dispersion). This paper evaluates accuracy and efficiency of recently developed *modal-pushover-based-scaling* (MPS) method to scale ground motions for tall buildings. The procedure presented explicitly considers structural strength and is based on the standard intensity measure (IM) of spectral acceleration in a form convenient for evaluating existing structures or proposed designs for new structures. Based on results presented for two actual buildings (19- and 52-story), it is demonstrated that MPS procedure provided a highly accurate estimate of the engineering demand parameters (EDPs), accompanied by significantly reduced record-to-record variability of the responses. In addition, the MPS procedure is shown to be much superior to the scaling procedure specified in the ASCE/SEI 7-05 document.

INTRODUCTION

For tall buildings with unusual configurations, innovative structural systems and high performance materials, the California Building Code (CBC) (ICBO, 2007) and ASCE/SEI 7-05 (ASCE, 2005) documents permit the use of "alternate materials and methods of construction" relative to those prescribed in their seismic requirements with the approval of the regulatory agency. For these buildings, performance-based seismic design (PBSD) concepts are being increasingly employed to ensure their safety, constructability, sustainability and affordability. PBSD often requires nonlinear RHA to validate prescribed performance objective which is generally *collapse prevention* for tall buildings under a very rare earthquake with a long recurrence interval, on the order of 2,475 years (Lew

[a] United States Geological Survey, Menlo Park, CA, ekalkan@usgs.gov
[b] University of California Berkeley, Berkeley, CA, chopra@ce.berkeley.edu

et al., 2008). The ground motions developed for very rare earthquakes are dominated by aleatoric (i.e., source) uncertainties because the strong ground motions recorded from large magnitude earthquakes are scarce. Thus, there is a great need to establish rational procedures for selecting and scaling records to match the target design spectrum.

Procedures for selecting and scaling ground motion records for a site-specific seismic hazard are broadly described in building codes, and have been the subject of considerable research in recent years. Current performance-based seismic design and evaluation methodologies (e.g., ASCE/SEI 7-05) prefer intensity-based ground motion scaling where the scaling factor for a ground motion record can be chosen to minimize the difference between its elastic response spectrum and the target spectrum over a period range $0.2T_1$ to $1.5T_1$ (T_1 = fundamental vibration period of the building). Since this method does not consider explicitly the inelastic behavior of the structure, it may not be appropriate for near-fault sites where the inelastic deformation can be significantly larger than the deformation of the corresponding linear system. For such sites, scaling methods that are based on the inelastic deformation spectrum or consider the response of the first-"mode" inelastic single-degree-of-freedom (SDF) system become more appropriate (Bazzurro and Luco 2004; Luco and Cornell, 2007; Tothong and Cornell, 2008; PEER, 2009).

Kalkan and Chopra (2010a,b) utilized these concepts to develop a *modal-pushover-based-scaling* (MPS) procedure for selecting and scaling earthquake ground motion records in a form convenient for evaluating existing structures and proposed designs of new structures. The objective of MPS is to determine scale factors for a small number of appositely selected records so that the nonlinear RHA of a structure subjected to these scaled records is accurate [i.e., accurately estimates the median values of the engineering demand parameters (EDPs) such as member forces, member deformations or story drifts] and is efficient [i.e., minimizes the number of records needed to reliably obtain these EDP estimates]. In contrast to the ASCE/SEI 7-05 scaling method, the MPS procedure explicitly considers structural strength obtained from the first-"mode" pushover curve, and determines a scaling factor for each record to match a target value of the deformation of the first-"mode" inelastic SDF system. Appropriate for first-"mode" dominated structures; this approach is extended for structures with significant contributions of higher modes. MPS is based on the standard intensity measure (IM) of spectral acceleration that is directly available from the USGS seismic hazard maps, where it is mapped for periods of 0.2 s and 1.0 s for the entire U.S. to facilitate construction of site-specific design spectrum, or it can be computed from the uniform hazard spectrum obtained by probabilistic or deterministic seismic hazard analysis for a given site. Thus, the MPS procedure does not require attenuation relations for any other IM.

The MPS procedure has been proven to be accurate and efficient for determining seismic demands due to one-horizontal component of ground motion for low- and medium-rise buildings, where the first-”mode” of vibration generally dominates their response (Kalkan and Chopra, 2010a,b). This paper investigates the accuracy and efficiency of the MPS procedure for nonlinear RHA of tall buildings where higher-mode effects generally have larger contribution to response. In addition, the accuracy and efficiency of the scaling procedure recommended in the ASCE/SEI 7-05 document is evaluated.

MODAL-PUSHOVER-BASED SCALING PROCEDURE: SUMMARY

The MPS procedure scales each record by a factor such that deformation of the first-“mode” inelastic SDF system—established from the first-“mode” pushover curve for the building—due to the scaled record matches a target value (Kalkan and Chopra, 2010a). Defined as the median deformation of the first-“mode” inelastic SDF system due to a large ensemble of unscaled ground motions compatible with the site-specific seismic hazard, the target deformation may be estimated by either (1) performing nonlinear RHA of the inelastic SDF system to obtain the peak deformation due to each ground motion, and then computing the median of the resulting data set; or (2) multiplying the median peak deformation of the corresponding linear SDF system, known from the median response spectrum, by the inelastic deformation ratio, estimated from an empirical equation (e.g., Chopra and Chintanapakdee, 2004).

For first-”mode” dominated structures, this version of the MPS procedure has been shown to be sufficient (Kalkan and Chopra, 2010a,b). Because high vibration modes are known to contribute significantly to the seismic response of tall buildings, the MPS procedure checks for second-”mode” compatibility of each record by comparing its scaled elastic spectral displacement response values at the second-”mode” vibration period of the structure against the target spectrum. This approach ensures that each scaled earthquake record satisfies two requirements: (1) the peak deformation of the first-”mode” inelastic SDF system is close enough to the target value of its inelastic deformation; and (2) the peak deformation of the second-”mode” (i.e., second-”mode”) elastic SDF system is not far from the target spectrum. The procedure has been summarized as a sequence of steps in Kalkan and Chopra (2010a).

GROUND MOTION ENSEMBLE

A total of twenty one near-fault strong earthquake ground motions were compiled from the Next Generation Attenuation project ground motion database. These motions were recorded during seismic events with moment magnitude M $\geq$ 6.5 at closest fault distances $R_{cl} \leq 12$ km and belonging to NEHRP site classification C and D. The selected ground motion records and their characteristic parameters are listed in Table 1. Because the twenty-one ground motions selected were not intense enough to drive the buildings considered far into the inelastic range—an obvious requirement to test any scaling procedure—they were amplified by a factor of 3.0; the resulting twenty-one ground motions are treated as "unscaled" records for this investigation. Shown in Figure 1 are the 5%-damped median response spectra of the "unscaled" ground motions. The median spectrum is taken as the design spectrum for purposes of evaluating the MPS and ASCE/SEI 7-05 scaling methods; also shown in this figure is the median spectrum of the ground motion ensemble as a four-way logarithmic plot, together with its idealized version (dashed-line). The idealized spectrum is divided into three period ranges: the long-period region to the right of point *d*, $T_n > T_d$, is called the displacement-sensitive region; the short-period region to the left of point *c*, $T_n < T_c$, is called the acceleration-sensitive region; and the intermediate-period region between points *c* and *d*, $T_c < T_n < T_d$, is called the velocity-sensitive region (Chopra, 2007; Section 6.8). Note that the nearly constant velocity region is unusually narrow, which is typical of near-fault ground motions.

BUILDINGS SELECTED, MODELING AND VALIDATION

The buildings selected to evaluate the efficiency and accuracy of the MPS method are existing 19- and 52-story steel special moment resisting frame buildings representative of tall building types in California. Both buildings are instrumented, and their recorded motions during past earthquakes were utilized to validate the computer models.

19-STORY BUILDING

The building shown in Figure 2 is located in Century City – Los Angeles, designed in 1966-67 and constructed in 1967. It has 19 stories above ground and 4 stories of parking below the ground level. The vertical load carrying system consists of 11.4 cm thick reinforced concrete slabs supported on steel beams. There is no composite action between the slab and steel beams due to lack of shear studs. The lateral load resisting system consists of four ductile steel moment frames in the longitudinal direction and five X-braced frames in the transverse direction. Moment resisting connections are used at the intersection of beams and columns. Perimeter columns are standard I-sections except at the first story where columns are built-up box-sections. The foundation system consists of 22 m long driven steel I-beam piles, capped in groups and connected by 61 cm square reinforced concrete tie beams.

The building was initially instrumented with only three sensors prior to the 1971 San Fernando earthquake, but 15 sensors were in place during the 1994 Northridge earthquake (Fig. 3). During the Northridge event (its epicenter was 20 km away from the site), the recorded peak horizontal accelerations were 0.32 g at the basement, 0.53 g at the ground floor and 0.65 g at the roof. This shaking caused moderate damage to the building in the form of buckling in some braces at upper floor levels in the transverse direction, but the perimeter moment frames were undamaged (Naeim, 1997).

A 3-D computer model of the building was developed for the superstructure above the ground level i.e., first-floor in Figure 3. Steel columns, beams, and braces were modeled by force-based nonlinear beam-column element in the open source finite element platform (OpenSees, 2006). To properly model the buckling response of the brace, a slight imperfection is introduced at the brace's mid-span. Centerline dimensions were used in element modeling. The building weight, including estimates of non-structural elements such as partition walls and the mechanical equipment in the roof, was estimated to be 102,309 kN. Nodes at each floor were constrained to have the same lateral displacement to simulate rigid diaphragm behavior. The estimated floor mass and mass moment of inertia were lumped at the centre of mass at each floor. Panel zone deformations and local connection fracture were not considered therefore modeling of members and connections was based on the assumption of stable hysteresis loops derived from a bilinear stress-strain model with 3% strain hardening. The expected yield stress for steel members equal to 250 MPa was used. The columns were assumed to be fixed at the first-floor, assumed as the base. P-Δ effects were included in the global system level.

The first six natural vibration periods of the building are identified by frequency domain analysis of the motion of the roof relative to base motion recorded during the Northridge event. Period computed from the computer model are close to identified values (Table 2). The two constants in Rayleigh damping were selected to provide damping ratios of 3% for the first and sixth modes. Nonlinear RHA of the building subjected to the two horizontal components of the motion recorded at the base level during the Northridge event leads to the relative displacement response in two horizontal directions at the roof, eight and second floors shown in Figure 4, where it is compared with the motions derived from records. The excellent agreement between the computed and recorded displacements indicates that the computer model is adequate.

52-STORY BUILDING

The second building selected, the eight tallest building (219 m) in downtown Los Angeles, was designed in 1988 and constructed in 1988–90. This building comprises a 52-story steel frame office tower and five levels of basement as underground parking. The floor plans of the tower are not perfectly square; the tip of every corner is clipped and the middle third of each side is notched. In groups of about five stories, above the 36th story, the corners of the floors are clipped further to provide a setback (Fig. 2).

The structural system of the building is composed of a braced-core, twelve columns (eight on the perimeter and four in the core), and eight 91.4 cm deep outrigger beams at each floor connecting the inner and outer columns. The core, which is about 17 m by 21 m, is concentrically braced between the level-A (the level below the ground-level) and the 50th storey. Moment resisting connections are used at the intersection of beams and columns. The outrigger beams, about 12 m long, link the four core columns to the eight perimeter columns to form a ductile moment resisting frame. The outrigger beams are laterally braced to prevent lateral torsional buckling and are effectively connected to the floor diaphragm by shear studs to transmit the horizontal shear force to the frame. Perimeter columns are standard I-sections, while the core columns are built-up sections with square cross section at the lower floor and crucifix section at the upper floors. The interior core is concentrically braced. The building foundation consists of concrete spread footings supporting the steel columns with 13 cm thick concrete slab on grade.

The building is instrumented with twenty accelerometers to record its translational and torsional motions (Fig. 5). During the Northridge earthquake (its epicenter was 30 km away from the site), the recorded values of peak horizontal accelerations were 0.15 g at the basement, 0.17 g at the level-A, and 0.41 g at the roof; no structural damage was observed (Ventura and Ding, 2000). The latest recorded event, the 2008 Chino-Hills earthquake (its epicenter is 47 km away from the site), generated a PGA of 0.06 g at the ground and 0.263 g at the roof level.

The 3-D model of the 52-story building in OpenSees included 58 separate column types and 23 different beam types. The building weight, including non-structural elements such as partition walls and the mechanical equipment in the roof, was estimated to be 235,760 kN. The material model is based on stable hysteresis loops derived from a bilinear stress-strain model with 2% strain hardening. All steel framing including columns are ASTM A-572 (grade 50) with a nominal yielding strength of 345 MPa.

The first nine natural vibration periods of the building identified from the recorded relative roof motions with respect to base during the Northridge and Chino-Hills events. The computer model was able to match the measured periods reasonably well (Table 2). Two coefficients of Rayleigh damping were selected to provide damping ratio of 4% for the first and ninth modes. Nonlinear RHA of the building subjected to the three components of the motion recorded at the base level during the Northridge event leads to the relative displacement response in two horizontal directions at the roof, 35th, 22nd, and 14th floor shown in Figure 6. The excellent agreement between the computed and recorded displacements indicates that the computer model is satisfactory. Further details of validation studies are available in Kalkan and Chopra (2010a).

FIRST-”MODE” SDF-SYSTEM PARAMETERS

The force-deformation relation for the first-”mode” SDF system for each building is determined from the base shear – roof displacement relation defined by the first-”mode” pushover curve, as described by the Step 5 of the MPS procedure. For both nominally symmetric buildings, only the E-W direction is considered in the pushover analysis (see Figs. 3 and 5). The resulting force-deformation relations for the first-”mode” SDF system are shown in Figure 7. For the 19-story building, a bilinear hysteretic force-deformation relation is found to be adequate, while for the 52-story building, the hysteretic force-deformation relation is idealized by the peak-oriented model (Ibarra et al., 2005) with the monotonic curve idealized as tri-linear.

EVALUATION OF MPS PROCEDURE

The accuracy of the MPS procedure was evaluated by comparing the median (defined as the geometric mean) value of an EDP due to a set of randomly selected seven scaled ground motions against the benchmark value, defined as the median value of the EDP due to the twenty-one “unscaled” ground motions. A scaling procedure is considered to be efficient if the dispersion of an EDP due to the set of seven scaled ground motions is small. Results are presented for three sets of seven ground motions that were randomly selected from the twenty-one ground motions.

BENCHMARK RESULTS

Figure 8 shows the benchmark EDPs for the two buildings: maximum values of floor displacements (normalized by building height), story drift ratios (story drift ÷ story height), and plastic rotations of the beams and columns. Results from individual records are also included to demonstrate the large dispersion or record-to-record variability. The peak values of story drift ratios range from 1.2% to 12.5% for the 19-story building, and 0.4% to 5.8% for the 52-story building. Almost all of the excitations drive both buildings well into the inelastic range as shown in Figure 9, where the roof displacement values due to the twenty-one "unscaled" ground motions are identified on the first-"mode" pushover curve; also shown is the median value. The median deformation exceeds the yield deformation by factors of 3.3 and 2.6, respectively for the 19- and 52-story buildings.

TARGET VALUE OF INELASTIC DEFORMATION

In evaluations of the MPS, "exact" value of first-"mode" target inelastic spectral displacement (i.e., $\bar{D}_1^I$) was assumed to be unknown and it was estimated using an empirical C_R equation (Chopra and Chintanapakdee, 2004). This estimate is compared in Figure 10 against the "exact" value of $\bar{D}_1^I$ (dashed horizontal line) determined by nonlinear RHAs of the first-"mode" inelastic SDF system for twenty-one "unscaled" records; values from individual records are also included to show its record-to-record variability. The empirical equation for C_R overestimates "exact" value of $\bar{D}_1^I$ by only 8% for the 19-story building, and under estimates "exact" value of $\bar{D}_1^I$ by only 1% for the 52-story building.

COMPARISONS AGAINST BENCHMARK RESULTS

Once $\bar{D}_1^I$ is estimated, an appropriate scale factor for each record is determined by implementing Steps 7-8 of the MPS procedure (i.e., considering first-"mode" only), and presented in Table 3; the scaling factors obviously differ with the building. The EDPs determined by nonlinear RHAs due to three sets of seven ground motions scaled according to the MPS procedure are compared against the benchmark EDPs in Figures 11 and 12 respectively for the 19- and 52-story buildings. Also included are the EDP values due to each of the scaled ground motions to show dispersion of the data. The values of EDPs due to a small (7) subset of scaled ground motions are close to the benchmark results. The median values of the peak floor displacements, story drift ratios and column plastic rotations are well estimated. The height-wise average errors in estimating the median values of peak floor displacements and drifts are 7% and 3%, respectively for the 19-story building, 9% and 8%, respectively for the 52-story building. These are the errors averaged over GM Sets 1-3.

The dispersion of the EDP values due to the seven scaled records is reduced as compared to the dispersion associated with the original records (Fig. 8), but this reduction is less at intermediate and upper floors, suggesting that second-”mode” responses should also be considered in the MPS procedure.

MPS CONSIDERING SECOND-”MODE”

Next, the second vibration “mode” is considered in selecting the most appropriate set of seven ground motions out of the twenty-one records scaled based on the first-”mode” response only by implementing Steps 10-13 of the MPS method. The seven records with the highest ranks (see Step 12) were defined as Ground Motion Set 4; this set is different for each building (see Table 4).

Figure 13 compares the median EDPs from ground motions scaled by the MPS method with the benchmark values for the two buildings. Considering the second-”mode” in selecting ground motions provides a more accurate estimate of the median EDPs; the height-wise average errors in estimating the median values of peak floor displacements and drift ratios are reduced to 6% and 2%, respectively for the 19-story building, 6% and 7%, respectively for the 52-story building. The height-wise average errors in beam plastic rotations are reduced from 34% (averaged over GM Sets 1-3) to 15% for GM Set 4 for the 52-story building where higher-mode contributions to response are more pronounced; however, the errors in case of the 19-story building remain essentially unchanged. For both buildings considering the second-”mode” in ground motion selection significantly reduces record-to-record variability (compared to the results achieved by Ground Motion Sets 1-3 as shown in Figs. 11 and 12). The enhanced accuracy and efficiency are demonstrated in Figure 14, where the Δ and σ—the median value of the ratio of the estimated story drift to its benchmark value, and dispersion of this ratio—are plotted for the four sets of ground motions. Ground Motion Set 4 is more accurate (i.e., height-wise distribution of Δ is in average closer to unity) and efficient (i.e., σ is closer to zero) than Ground Motion Sets 1 though 3.

COMPARING MPS AND CODE-BASED SCALING PROCEDURES

The EDPs determined by nonlinear RHA of the structure due to a set of seven ground motions scaled according to the ASCE/SEI 7-05 scaling method are compared against the benchmark EDPs. Figures 15 and 16 present such comparisons for the two buildings and for the three sets of seven ground motions. The ground motions scaled according to the ASCE/SEI 7-05 scaling method overestimate the median EDPs with the height-wise average overestimation of floor displacements and story drifts by 15% and 10% respectively, for the 19-story building, 93% and 130% respectively, for the 52-story building; obviously this overestimation in the latter case is unacceptably large. Errors in beam and column plastic rotations are also considerable. As evident by comparing Figures 11-12 with Figures 15-16, the MPS method leads to much smaller dispersion compared to the ASCE/SEI 7-05 scaling method. The large dispersion associated with the ASCE/SEI 7-05 scaling method suggests that ground motion records should not be selected randomly from a large set of records that conforms to the site-specific hazard conditions (i.e., magnitude, distance and site geology), but their spectral shape should also be considered.

To demonstrate the importance of spectral shape of selected records on the accuracy and efficiency of the ASCE/SEI 7-05 scaling criteria, we deliberately selected a set of seven records (out of twenty-one) such that their scaled spectral accelerations, $A(T_1)$ and $A(T_2)$ at the first two vibration periods of the building, T_1 and T_2, are significantly higher than the design spectrum; this final set is identified as Ground Motion Set 5. Figure 17 compares the average spectrum of scaled records in Set 5 with the design spectrum for the 19- and 52-story buildings; also shown are the individual spectra. For both buildings, the average value of $A(T_1)$ and $A(T_2)$ are significantly larger than the design spectrum values at these periods.

The median values of EDPs due to GM Set 5 are compared with the benchmark values in Figure 18 for the two buildings. Clearly the ASCE/SEI 7-05 scaling method grossly overestimates EDPs at almost all floors, e.g., floor displacements are overestimated by as much as 100% for the 19-story building, and almost 200% for the 52-story building. The dispersion in responses due to Ground Motion Set 5 is much larger compared to Sets 1-3. To obtain acceptable estimates of EDPs using records scaled by the ASCE/SEI 7-05 scaling method, the selected records must satisfy the requirement that their scaled response spectra are close to the design spectrum values at T_1 and T_2. In contrast, the MPS method (with scaling based on "first"-mode only) is effective in scaling the records in GM Set 5 to achieve good estimates of EDPs. This is demonstrated in Figure 19 where the floor displacements and story drifts differ from the benchmark results by less than 10%; however the errors in plastic hinge rotations are larger. It is reassuring to observe that the MPS procedure is effective in scaling even records with spectral shape significantly different than the design spectrum.

CONCLUSIONS

Selected for this investigation were actual 19- and 52-story symmetric-plan buildings with their computer models calibrated against their motions recorded during southern Californian earthquakes. This evaluation of the MPS procedure in estimating seismic demands for these two buildings has led to the following conclusions:

1. Even for the most intense near-fault ground motions, which represent a severe test, the MPS method estimates the median value of seismic demands to a good degree of accuracy (within 15% of the benchmark value) with dispersion of responses much smaller than for unscaled records in estimating seismic demands for tall buildings.
2. For tall buildings where higher vibration modes are known to contribute significantly to the seismic response, the MPS method requires an additional step to rank the scaled ground motions based on the closeness of the elastic deformation of second-”mode” elastic SDF systems to their target values. Selecting a subset of highest-ranked ground motions leads to a method that is more accurate and efficient for estimating seismic demands.
3. The MPS procedure is shown to be much superior compared to the ASCE/SEI 7-05 procedure for scaling ground motion records. This superiority is evident in two respects. First, the ground motions scaled according to the MPS procedure provide median values of EDPs that are much closer to the benchmark values than is achieved by the ASCE/SEI 7-05 procedure. The height-wise average discrepancy of over 30% in story drift ratios (relative to the benchmark values) determined by scaling records according to the ASCE/SEI 7-05 procedure is reduced to less than 15% when records are scaled by the MPS procedure. Second, the dispersion (or record-to-record variability) in the EDPs due to seven scaled records around the median is much smaller when records are scaled by the MPS procedure compared to the ASCE/SEI 7-05 scaling method.
4. The ASCE/SEI 7-05 scaling method is seriously deficient if the records selected based on earthquake magnitude, distance and site geology are such that their scaled spectral

acceleration at T_1 and T_2 significantly exceed the design spectrum values at these periods. However, the MPS procedure is effective in scaling even such records with spectral shape significantly different than the design spectrum.

ACKNOWLEDGMENTS

The first author would like to acknowledge the generous support of the Earthquake Engineering Research Institute for providing him the 2008 EERI/FEMA NEHRP Professional Fellowship in Earthquake Hazard Reduction to pursue a research to develop "*Practical Guidelines to Select and Scale Earthquake Records for Nonlinear Response History Analysis of Structures*". Complete report of this research study is available on line at http://nsmp.wr.usgs.gov/ekalkan/MPS/index.html.

REFERENCES

American Society of Civil Engineers (2005), ASCE/SEI 7-05: Minimum Design Loads for Buildings, Reston, VA.

Bobadilla, H. and A.K. Chopra (2007), Modal Pushover Analysis for Seismic Evaluation of Reinforced Concrete Special Moment Resisting Frame Buildings, Earthquake Engineering Research Center, EERC/2007-01, 68 p.

Bazzurro, P. and Luco, N. (2004). Parameterization of Non-Stationary Acceleration Time Histories. Lifelines Program Project 1G00 Addenda. Pacific Earthquake Engineering Research (PEER) Center, University of California: Berkeley, CA, 83 p.

Chopra, A. K. and Chinatanapakdee, C. (2004). "Inelastic Deformation Ratios for Design and Evaluation of Structures: Single-Degree-of-Freedom Bilinear Systems," *J. of Str. Eng*. (ASCE), Vol. 130, No. 9, pp. 1304-1319.

Chopra, A.K. (2007). Dynamics of Structures: Theory and Applications to Eq. Eng. Prentice Hall, Englewood Cliffs, N.J.

Han, S.W. and Chopra, A.K. (2006). "Approximate Incremental Dynamic Analysis using the Modal Pushover Analysis Procedure", *Eq. Eng. and Str. Dyn*., Vol. 35, pp. 1853-1873.

Ibarra, L., Medina, R. and H. Krawinkler, (2005). "Hysteretic models that incorporate strength and stiffness deterioration", *Eq. Eng. and Str. Dyn*., Vol. 34, pp. 1489-1511.

International Conference of Building Officials (2007). California Building Code, Whittier, CA.

Kalkan, E. and Chopra, A.K. (2010a) Practical Guidelines to Select and Scale Earthquake Records for Nonlinear Response History Analysis of Structures, USGS Open File Report No: 2010-1068, 126 p. (Available online at http://nsmp.wr.usgs.gov/ekalkan/MPS/index.html; last accessed on 05/2010).

Kalkan E., and Chopra A. K. (2010b) "Modal-Pushover-based Ground Motion Scaling Procedure", *J. of Str. Eng*. (ASCE), (in-press; available online at http://nsmp.wr.usgs.gov/ekalkan/PDFs/Papers/J25_Kalkan_Chopra.pdf; last accessed on 05/2010).

Lew, M., Naeim F., Hudson M.B., Korin B.O. (2008). "Challenges in Specifying Ground Motions For Design of Tall Buildings in High Seismic Regions of the United States", *Proc. of the 14th World Conference on Eq, Eng.*, October 12-17, 2008, Beijing, China.

Luco, N., and Cornell, A. C., (2007). "Structure-specific scalar intensity measures for near-source and ordinary earthquake ground motions", *Earthquake Spectra*, Vol. 23, No. 2, pp. 357-392.

Naeim, F. (1997), Performance of Extensively Instrumented Buildings during the January 17, 1994 Northridge Earthquake - An Interactive Information System, Report 7530.68/97, John A. Martin and Associates.

OpenSEES. Open Source finite element platform for earthquake engineering simulations (2006). University of California Berkeley, Pacific Earthquake Engineering Center. (Available online at http://opensees.berkeley.edu/; last accessed on 05/2010).

PEER Ground Motion Selection and Modification Working Group, (2009). Evaluation of Ground Motion Selection and Modification Methods: Predicting Median Interstory Drift Response of Buildings, Haselton, C.B. (editor). PEER Report 2009/01, University of California, Berkeley, CA.

Tothong, P. and Cornell, A.C. (2008). "Structural performance assessment under near-source pulse-like ground motions using advanced ground motion intensity measures", *Eq. Eng. and Str. Dyn*., Vol. 37, No. 7, pp. 1013-1037.

Ventura, C.E. and Ding, Y. (2000). "Linear and nonlinear seismic response of a 52-storey steel frame building", *The Structural Design of Tall Buildings*, Vol. 9, No. 1, pp. 25-45.

NOTATION

The following symbols are used in this paper:

A	=	Pseudo-spectral acceleration
C_R	=	Ratio of peak deformations of inelastic and corresponding elastic SDF systems for systems with known yield-strength reduction factor
D_n	=	Peak deformation of elastic SDF system for n^{th}-mode
$\bar{D}_1^I$	=	First-"mode" target value of inelastic spectral displacement
M	=	Moment magnitude of earthquake
n	=	Mode sequence number
R_{cl}	=	Closest distance to co-seismic rupture plane
T_c	=	Period separating acceleration and velocity-sensitive regions of the target spectrum
T_d	=	Period separating velocity and displacement-sensitive regions of the target spectrum
T_n	=	Elastic natural vibration period
V_{S30}	=	Average shear-wave velocity within 30m depth from surface
α	=	Ratio of post-yield and initial stiffness
ζ	=	Damping ratio
Δ	=	Geometric mean
σ	=	Dispersion

TABLE CAPTIONS

Table 1. Selected near-fault ground motions

Table 2. Measured and computed natural periods for 19- and 52-story buildings

Table 3. Scale factors for 19- and 52-story buildings and for three sets of seven ground motions

Table 4. Scale factors for 19- and 52-story buildings considering second-"mode"

FIGURE CAPTIONS

Figure 1. **(Left) Individual response spectra for twenty-one "unscaled" ground motions and their median response spectrum taken as the "design spectrum"; (Right) Median elastic response spectrum for the selected**

ensemble of ground motions shown by a solid line, together with its idealized version in dashed line; spectral regions are also identified; nearly constant velocity region is unusually narrow, which is typical of near-fault ground motions. Damping ratio, ζ= 5%.

Figure 2. **Overview of the 19-story (left) and 52-story (right) buildings located in Los Angeles County.**

Figure 3. **Instrumentation layout of the 19-story building.**

Figure 4. **Comparison of observed and computed floor displacements in two horizontal directions of the 19-story building at different floor levels; recorded data is from the M6.7 1994 Northridge earthquake. The excellent agreement between the computed (OpenSees) and recorded displacements indicates that the computer model is adequate.**

Figure 5. **Instrumentation layout of the 52-story building.**

Figure 6. **Comparison of recorded and computed floor displacements in two horizontal directions of the 52-story building at different floor levels; recorded data is from the M5.4 2008 Chino-Hills earthquake. The excellent agreement between the computed (OpenSees) and recorded displacements indicates that the computer model is satisfactory.**

Figure 7. **Comparison of first-"mode" pushover curve (solid line) and its idealized model (dashed line) for the 19- and 52-story buildings. For the 19-story building, a bilinear hysteretic force-deformation relation is found to be adequate, while for the 52-story building, the hysteretic force-deformation relation is idealized by the peak-oriented model with the monotonic curve idealized as tri-linear.**

Figure 8. **Median values of EDPs determined by nonlinear RHA of 19- (top row) and 52-story (bottom row) buildings for twenty-one "unscaled" ground motions; results for individual ground motions are also included to show significant record-to-record variability.**

Figure 9. **Roof displacements determined by nonlinear RHA of the 19- and 52-story buildings for twenty-one ground motions identified on first-"mode" pushover curves. The median deformation exceeds the yield deformation by factors of 3.3 and 2.6, respectively for the 19- and 52-story buildings.**

Figure 10. **Peak deformation D_1^I values of the first-"mode" inelastic SDF system for twenty-one "unscaled" ground motions for the 19- and 52-story buildings; "exact" target value of deformation $\bar{D}_1^I$ is identified by horizontal dashed line; horizontal continuous line indicates target value of deformation $\bar{D}_1^I$ established by the C_R equation. The empirical equation for C_R overestimates "exact" value of $\bar{D}_1^I$ by only 8% for the 19-story building, and under estimates "exact" value of $\bar{D}_1^I$ by only 1% for the 52-story building.**

Figure 11. **Comparison of median EDPs based on the MPS procedure with benchmark EDPs for the 19-story building; individual results for each of the seven scaled ground motions are also presented.**

Figure 12. **Comparison of median EDPs based on the MPS procedure with benchmark EDPs for the 52-story building; individual results for each of the seven scaled ground motions are also presented.**

Figure 13. **Comparison of median EDPs for Ground Motion Set 4 scaled according to MPS procedure with benchmark EDPs; individual results of seven scaled ground motions are also presented. Results are for the 19- (top row), and 52-story building (bottom row).**

Figure 14. **Median Δ_{MPS} and dispersion σ_{MPS} of story drift ratios for four ground motions sets and for 19-story and 52-story buildings.**

Figure 15. **Comparison of median EDPs based on the ASCE/SEI 7-05 ground motion scaling procedure with benchmark EDPs for the 19-story building; individual results for each of the seven scaled ground motions are also presented.**

Figure 16. **Comparison of median EDPs based on the ASCE/SEI 7-05 ground motion scaling procedure with benchmark EDPs for the 52-story building; individual results for each of the seven scaled ground motions are also presented.**

Figure 17. **Comparison of design spectrum with the average spectrum of seven scaled ground motions (GM Set 5) based on the ASCE/SEI 7-05 scaling method; individual response spectra are also presented. Spectral plots are for the 19- (left), and 52-story building (right). The average values of $A(T_1)$ and $A(T_2)$ from seven scaled records are much larger than the design spectrum values at these periods.**

Figure 18. **Comparison of median EDPs for Ground Motion Set 5 based on the ASCE/SEI 7-05 ground motion scaling procedure with benchmark EDPs for the 19-, and 52-story buildings; individual results for each of seven scaled ground motions are also presented. Results are for the 19- (top row), and 52-story building (bottom row).**

Figure 19. **Comparison of EDPs for Ground Motion Set 5 scaled according to MPS procedure (considering first-“mode” only) with benchmark EDPs; individual results for each of seven scaled ground motions are also presented. Results are for the 19- (top row), and 52-story building (bottom row).**

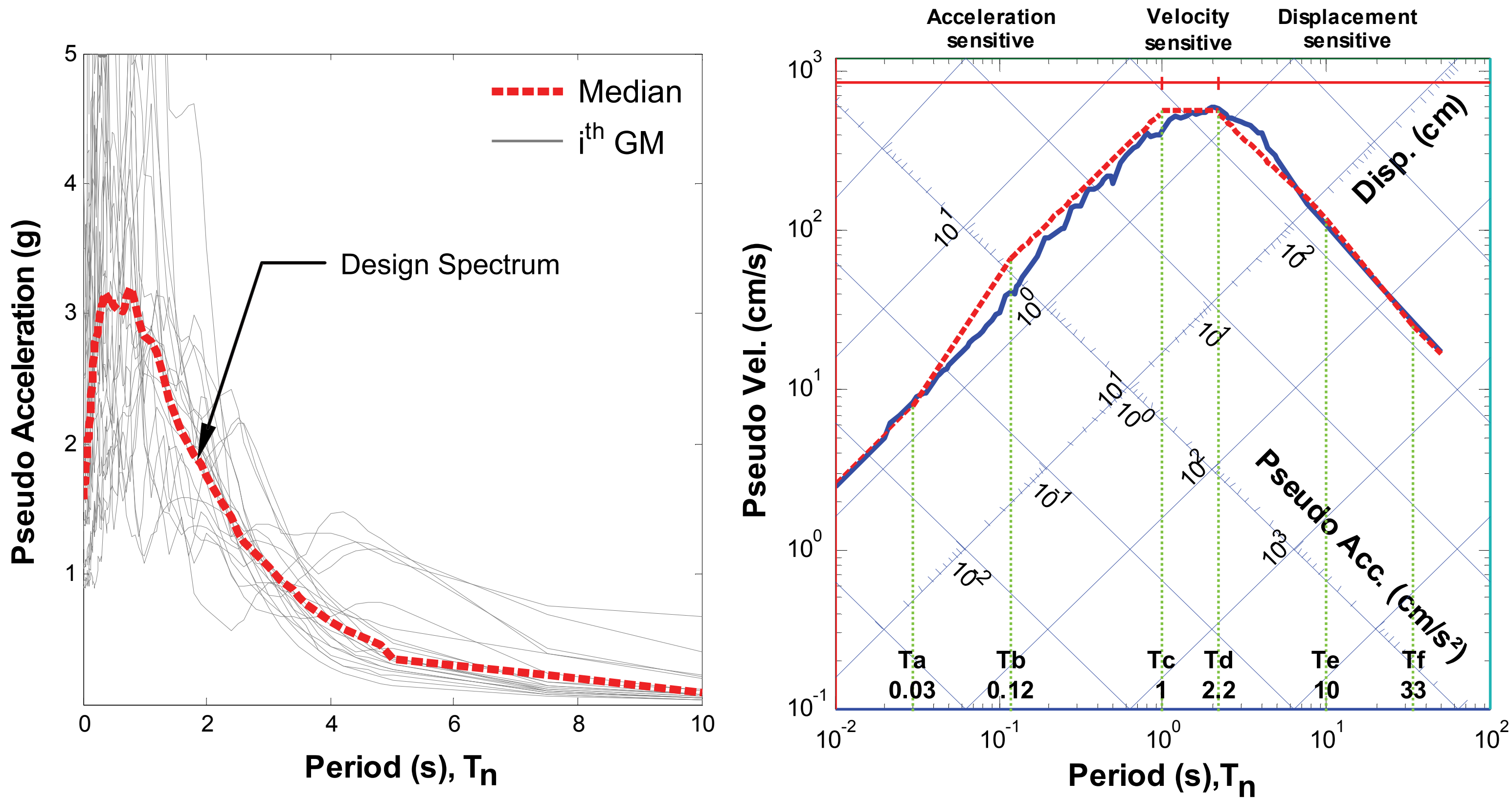
Pseudo Acceleration (g)
Median
ith GM
Design Spectrum
Period (s), Tn
Acceleration sensitive
Velocity sensitive
Displacement sensitive
Pseudo Vel. (cm/s)
Disp. (cm)
Pseudo Acc. (cm/s²)
Ta 0.03
Tb 0.12
Tc 1
Td 2.2
Te 10
Tf 33
Period (s),Tn

Figure - 1

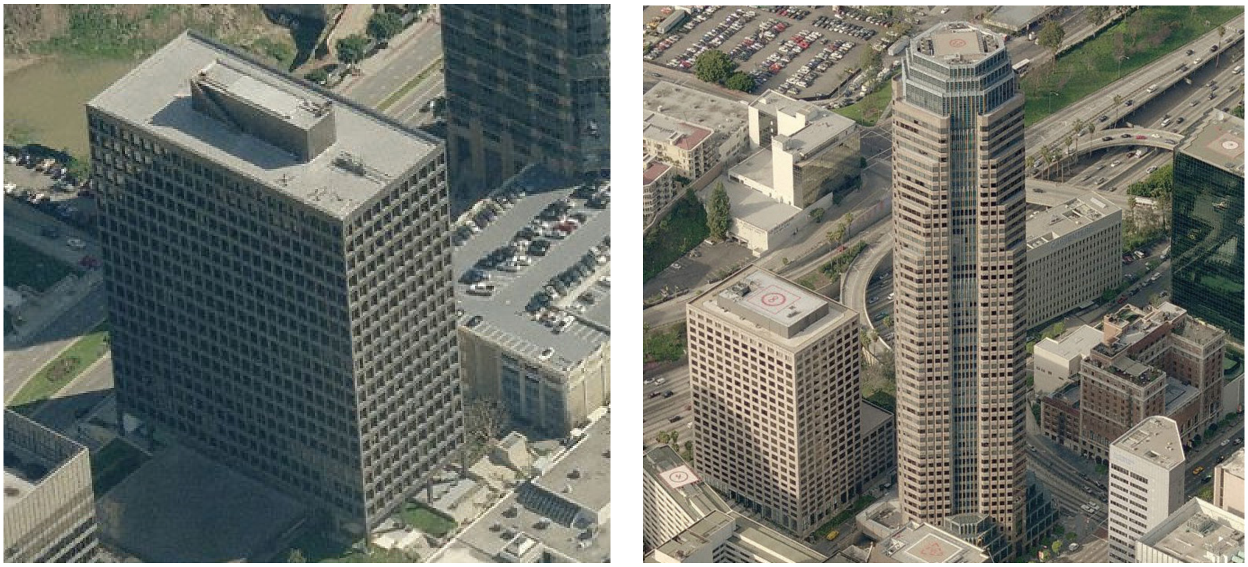

Figure - 2

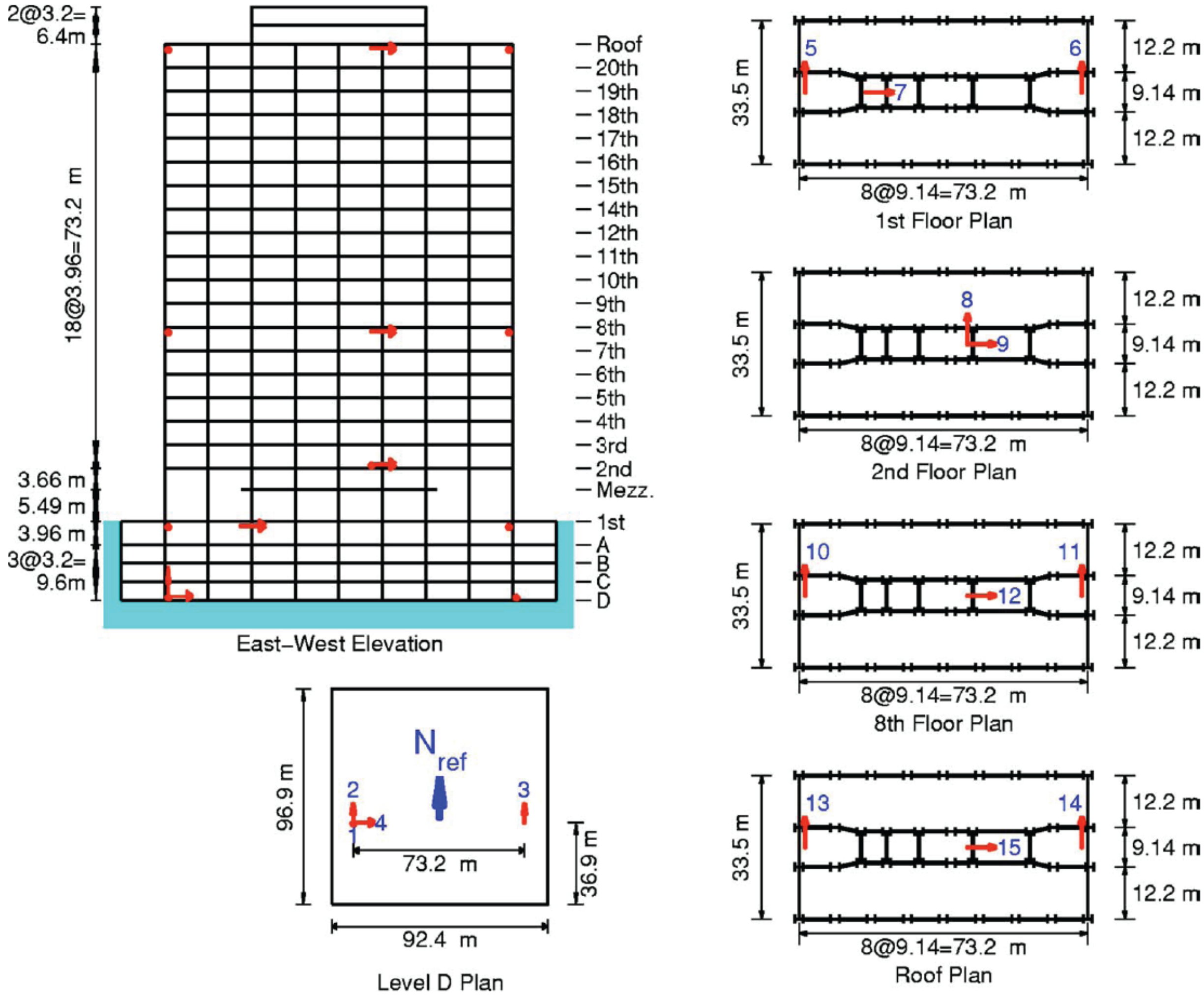
2@3.2=
6.4m
18@3.96=73.2 m
3.66 m
5.49 m
3.96 m
3@3.2=
9.6m
Roof
20th
19th
18th
17th
16th
15th
14th
12th
11th
10th
9th
8th
7th
6th
5th
4th
3rd
2nd
Mezz.
1st
A
B
C
D
East–West Elevation
96.9 m
N
ref
2
3
1
4
73.2 m
36.9 m
92.4 m
Level D Plan
33.5 m
5
6
7
12.2 m
9.14 m
12.2 m
8@9.14=73.2 m
1st Floor Plan
8
9
2nd Floor Plan
10
11
12
8th Floor Plan
13
14
15
Roof Plan

Figure - 3

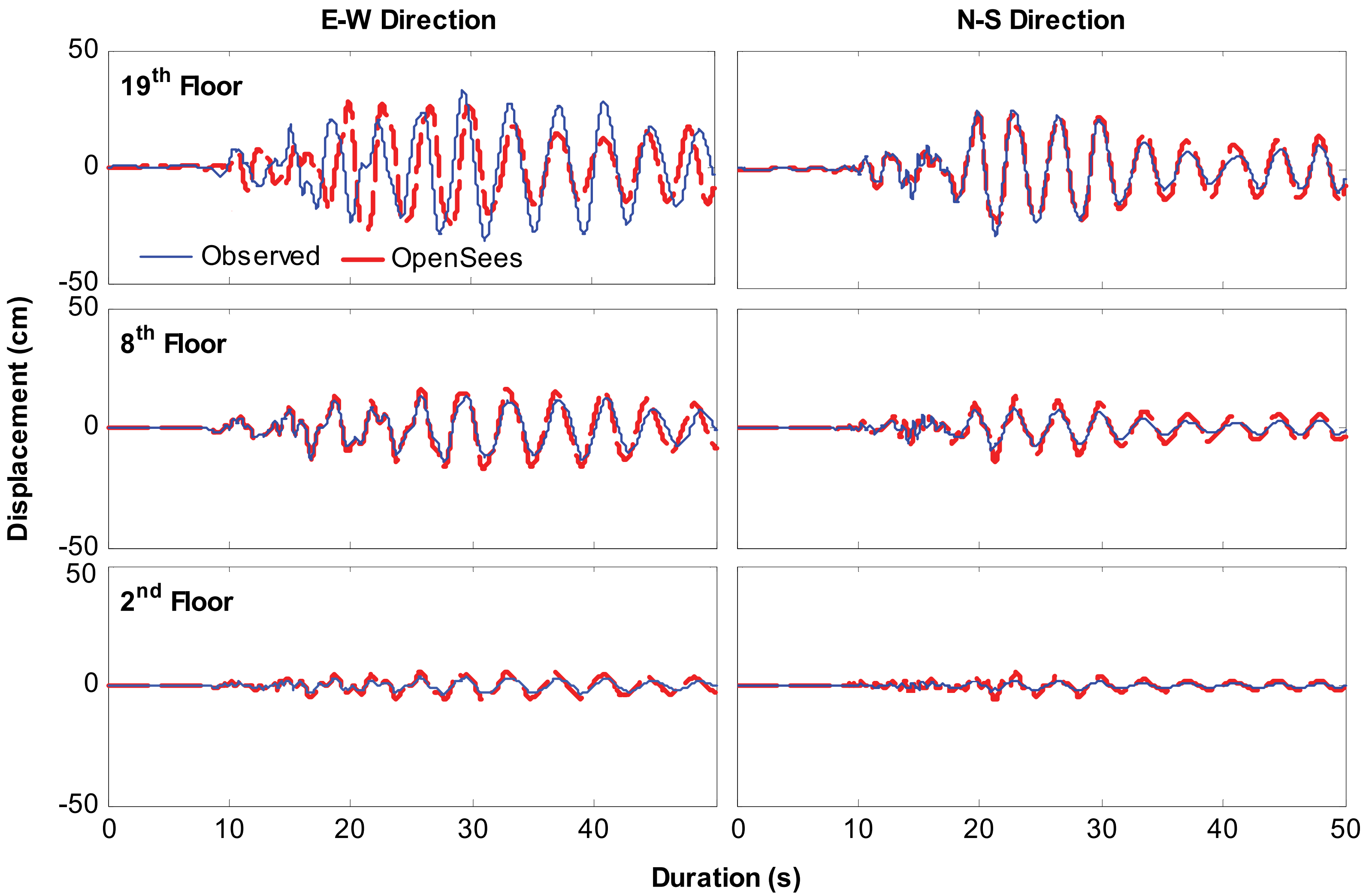
E-W Direction
N-S Direction
19th Floor
8th Floor
2nd Floor
Observed
OpenSees
Displacement (cm)
Duration (s)
50
0
-50
0
10
20
30
40
50

Figure - 4

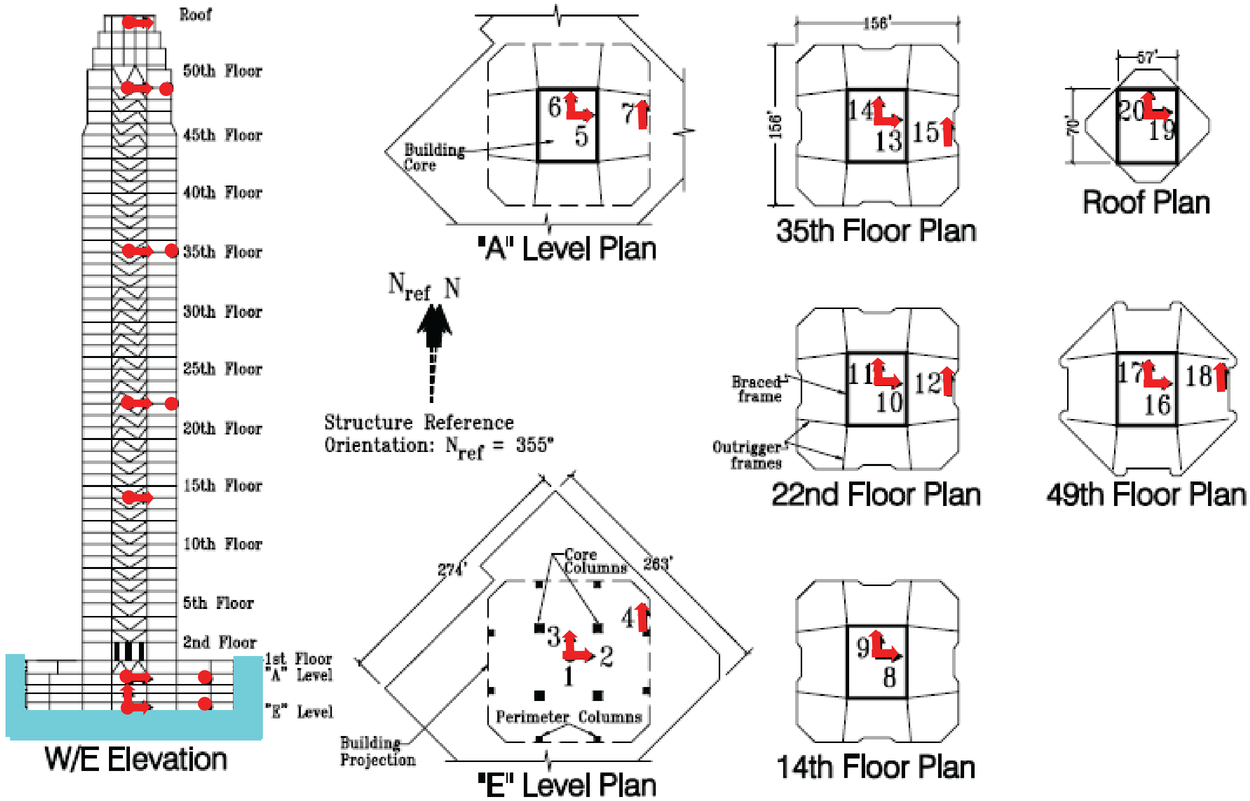
Roof
50th Floor
45th Floor
40th Floor
35th Floor
30th Floor
25th Floor
20th Floor
15th Floor
10th Floor
5th Floor
2nd Floor
1st Floor
"A" Level
"E" Level
W/E Elevation
6
5
7
Building Core
"A" Level Plan
Nref N
Structure Reference Orientation: Nref = 355°
274'
263'
Core Columns
3
2
1
4
Perimeter Columns
Building Projection
"E" Level Plan
156'
156'
14
13
15
35th Floor Plan
57'
70'
20
19
Roof Plan
Braced frame
Outrigger frames
11
10
12
22nd Floor Plan
17
16
18
49th Floor Plan
9
8
14th Floor Plan

Figure - 5

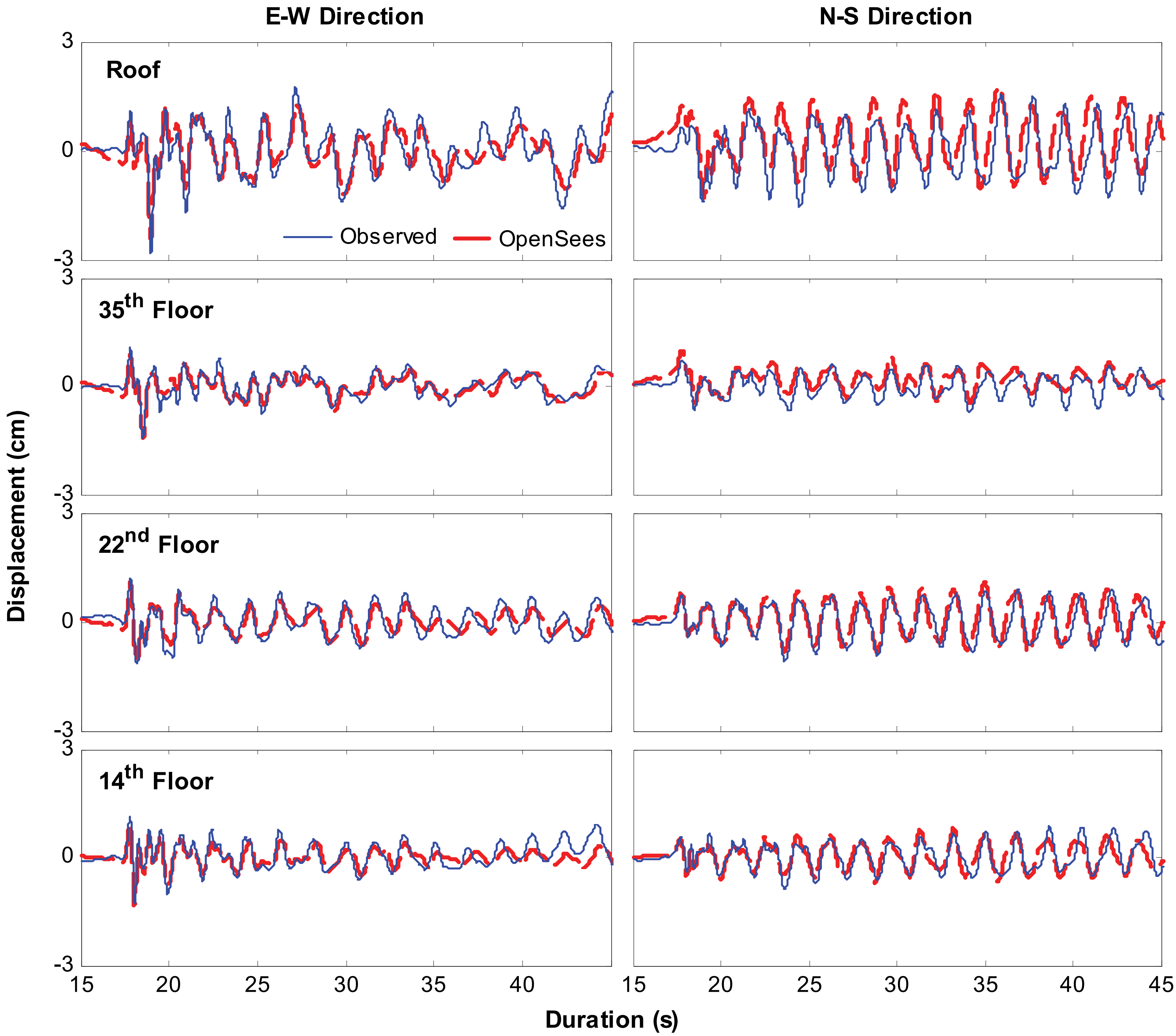

E-W Direction
N-S Direction
Roof
35th Floor
22nd Floor
14th Floor
Observed
OpenSees
Displacement (cm)
Duration (s)
3
0
-3
15
20
25
30
35
40
45

Figure - 6

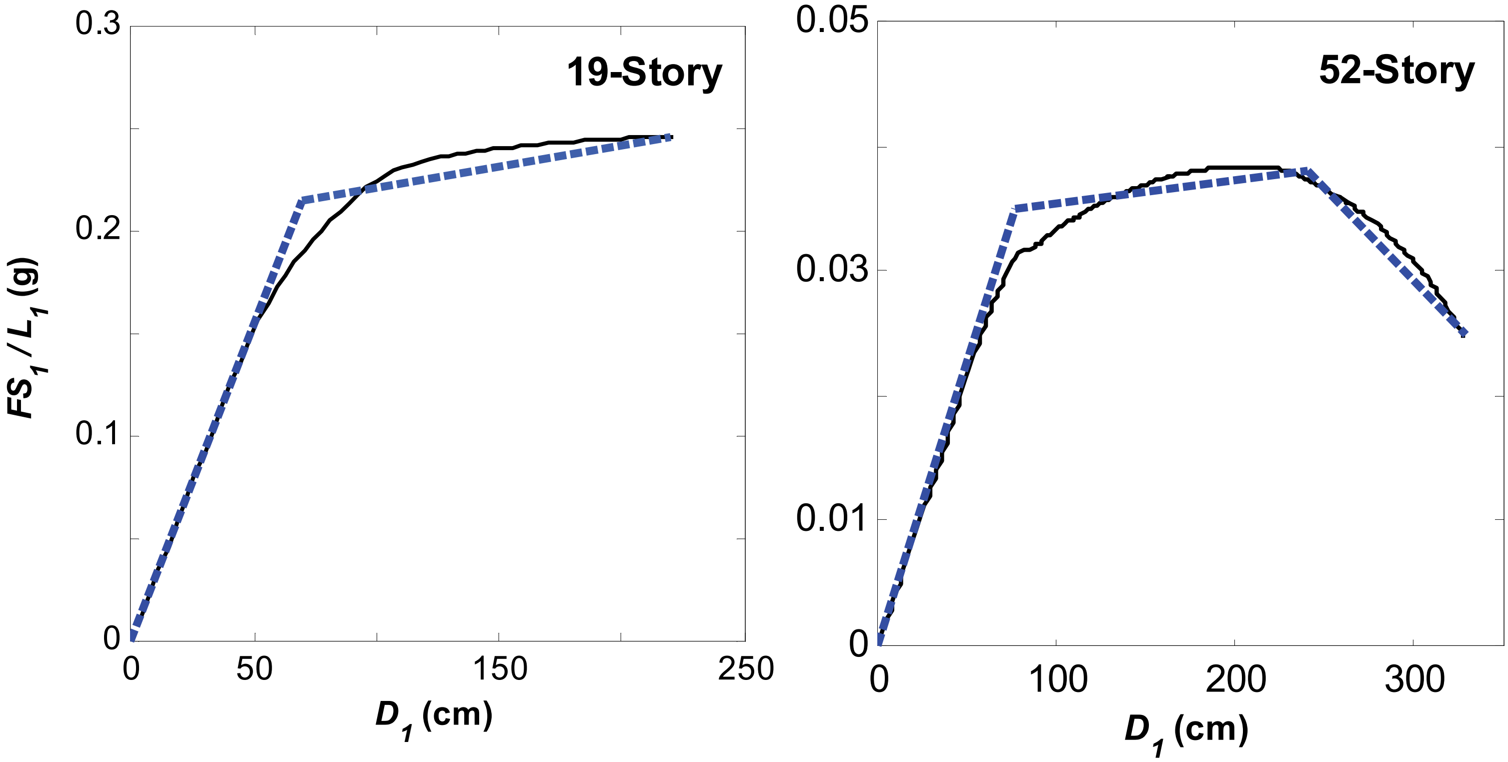
0.3
0.2
0.1
0
0
50
150
250
19-Story
FS_1 / L_1 (g)
D_1 (cm)
0.05
0.03
0.01
0
0
100
200
300
52-Story
D_1 (cm)

Figure - 7

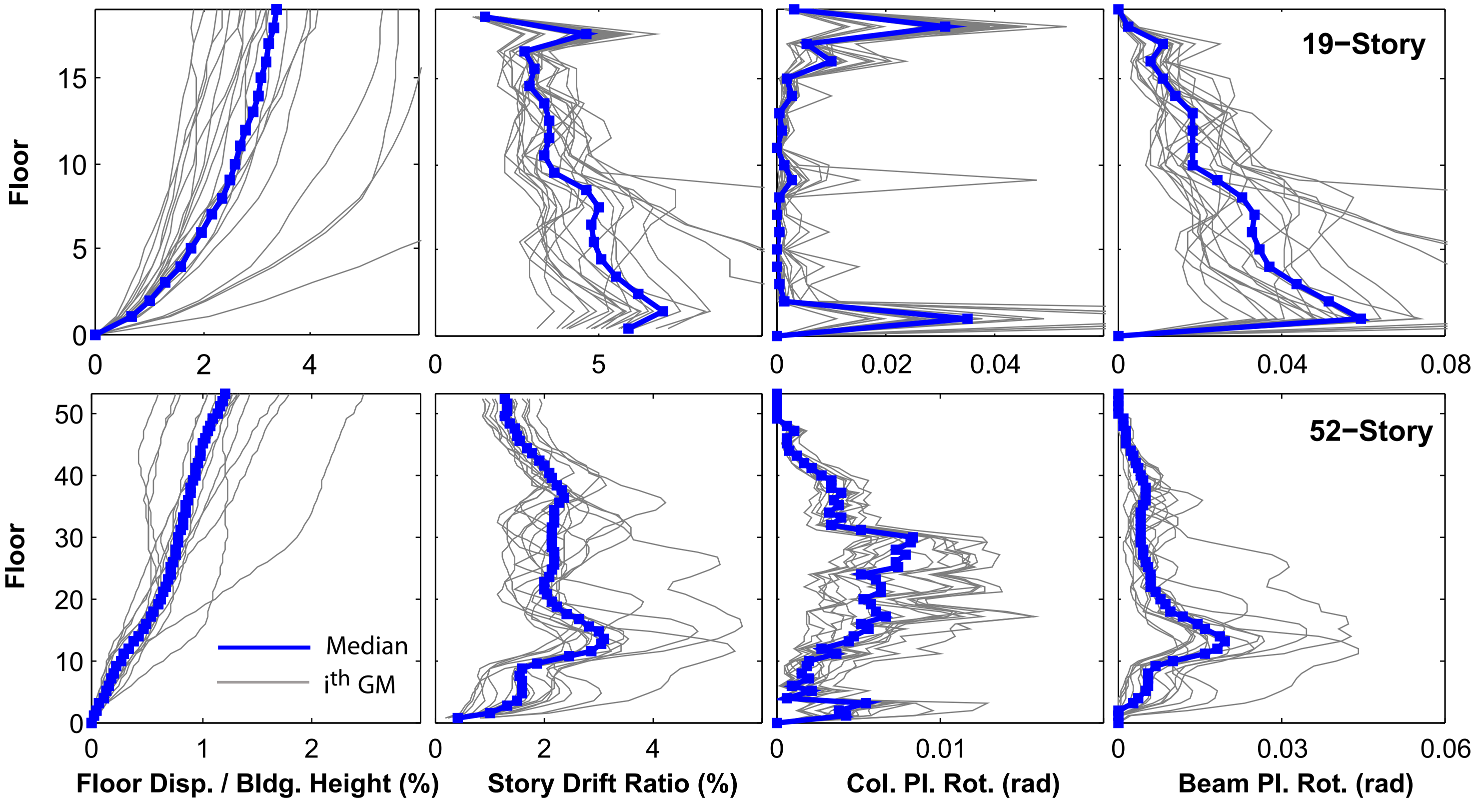

19−Story
52−Story
Floor
Floor
Median
i^th GM
Floor Disp. / Bldg. Height (%)
Story Drift Ratio (%)
Col. Pl. Rot. (rad)
Beam Pl. Rot. (rad)

Figure - 8

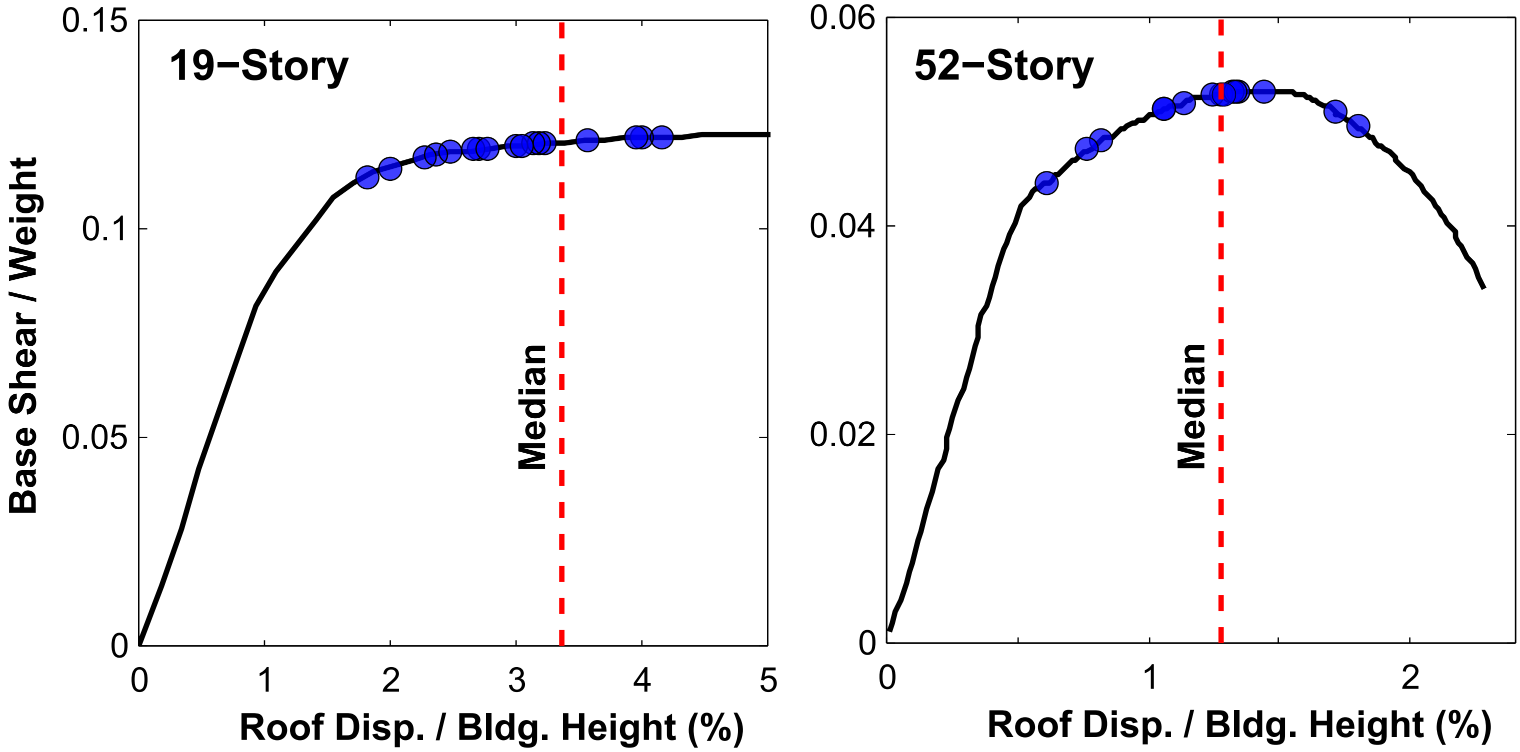

19−Story
Base Shear / Weight
0.15
0.1
0.05
0
Median
0
1
2
3
4
5
Roof Disp. / Bldg. Height (%)
52−Story
0.06
0.04
0.02
0
Median
0
1
2
Roof Disp. / Bldg. Height (%)

Figure - 9

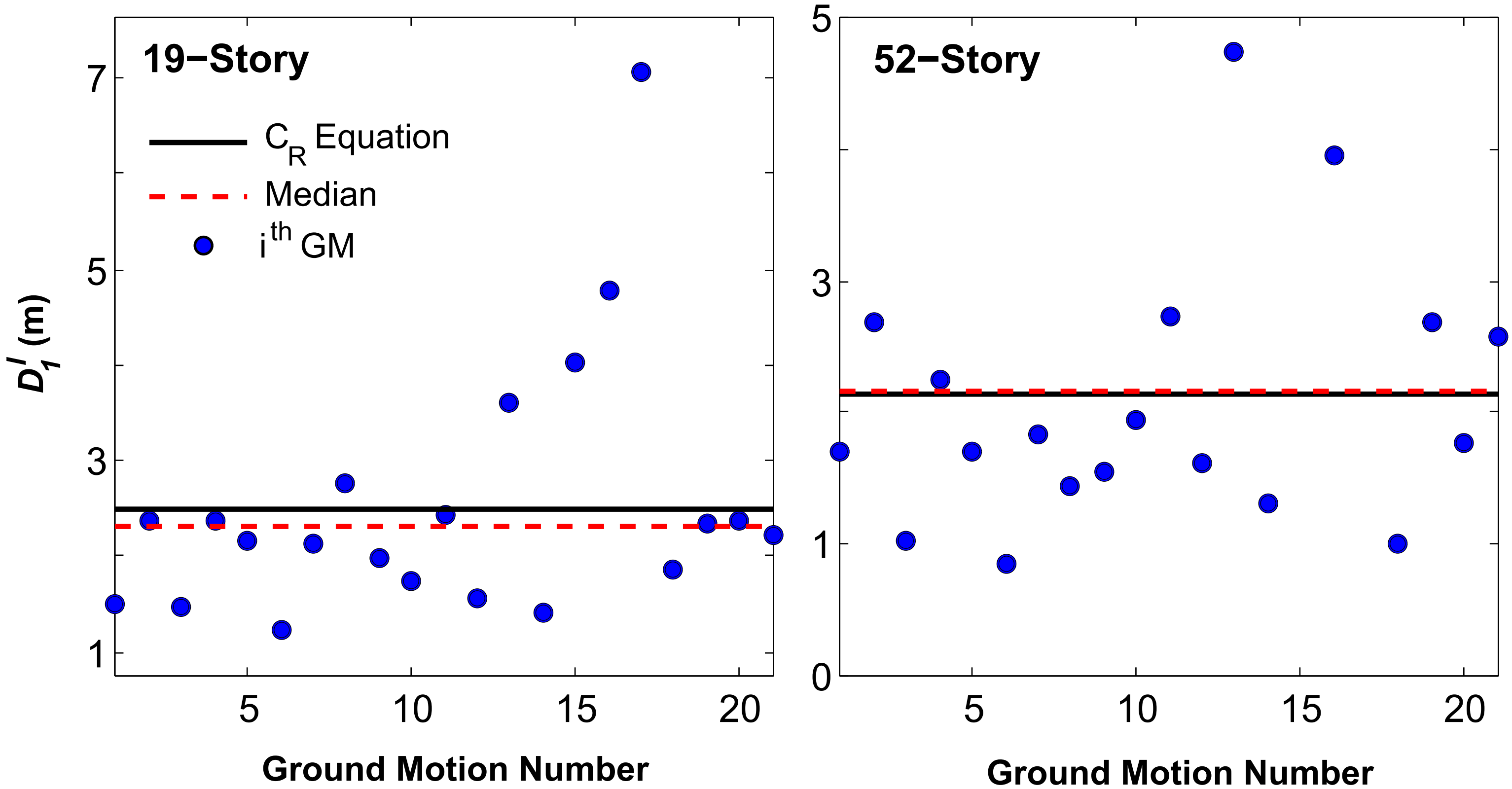

19−Story
52−Story
C_R Equation
Median
i^{th} GM
D_1^I (m)
Ground Motion Number
Ground Motion Number

Figure - 10

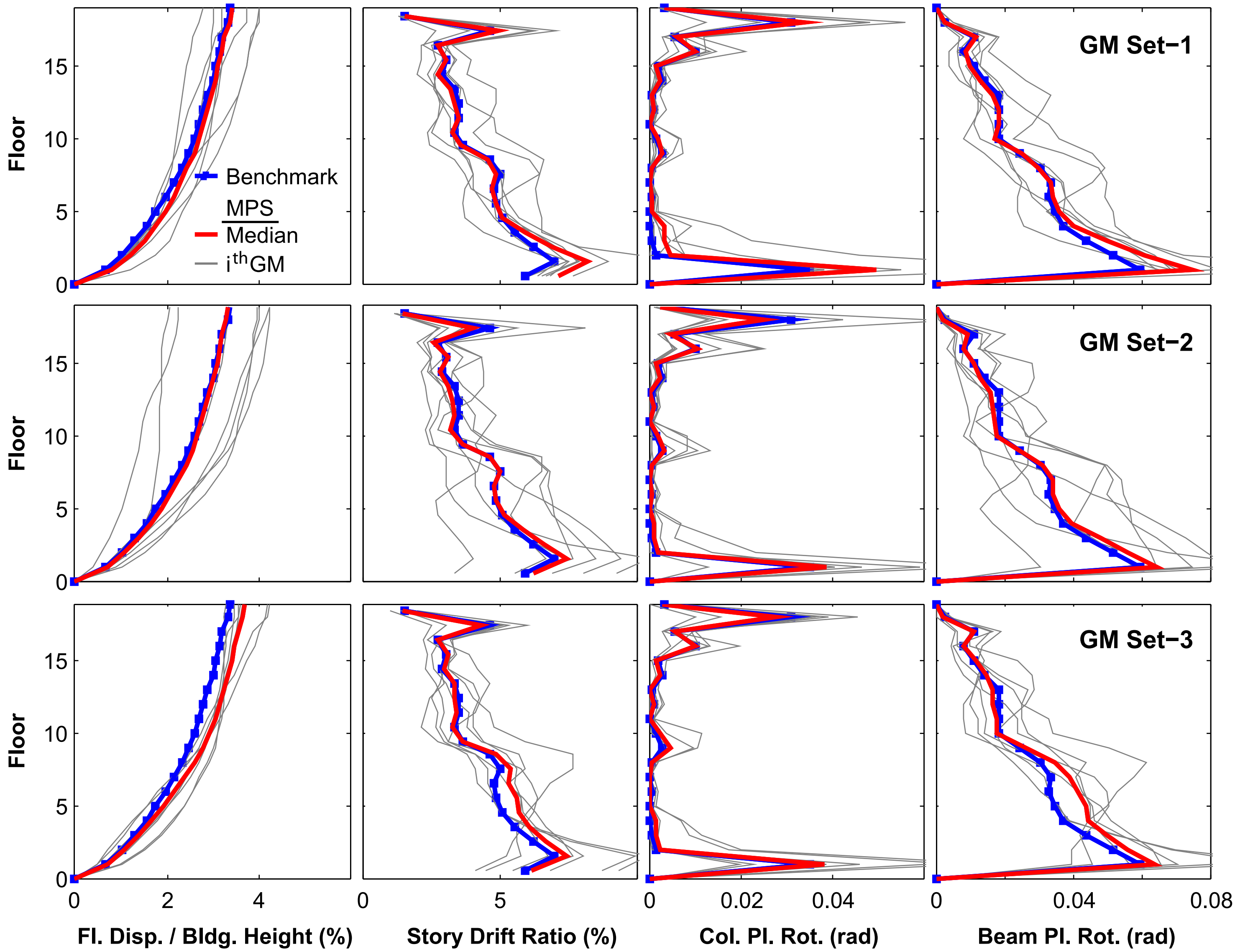
GM Set−1
GM Set−2
GM Set−3
Benchmark
MPS
Median
i^th GM
Floor
Fl. Disp. / Bldg. Height (%)
Story Drift Ratio (%)
Col. Pl. Rot. (rad)
Beam Pl. Rot. (rad)

Figure - 11

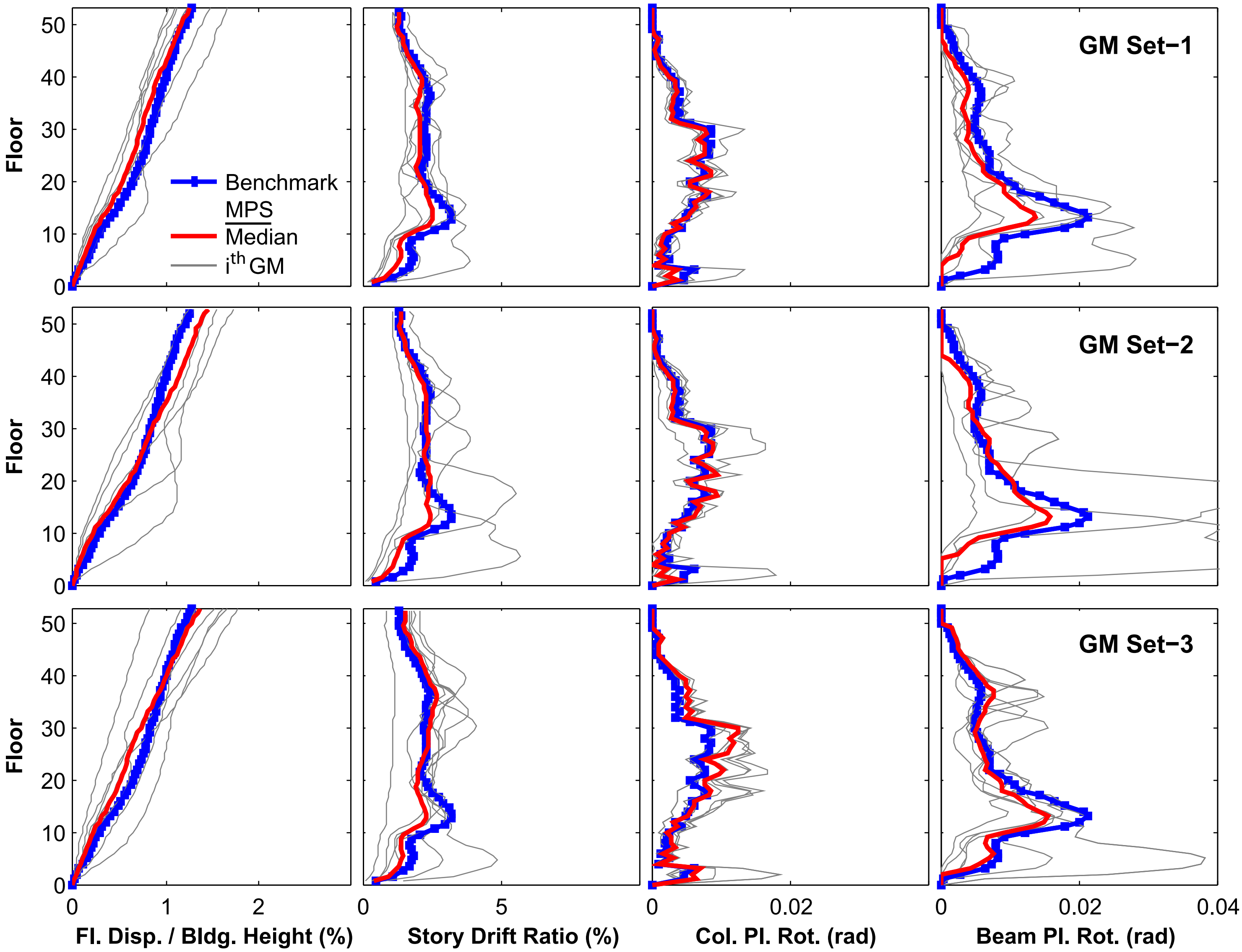
GM Set−1
GM Set−2
GM Set−3
Floor
Benchmark
MPS
Median
i^th GM
Fl. Disp. / Bldg. Height (%)
Story Drift Ratio (%)
Col. Pl. Rot. (rad)
Beam Pl. Rot. (rad)

Figure - 12

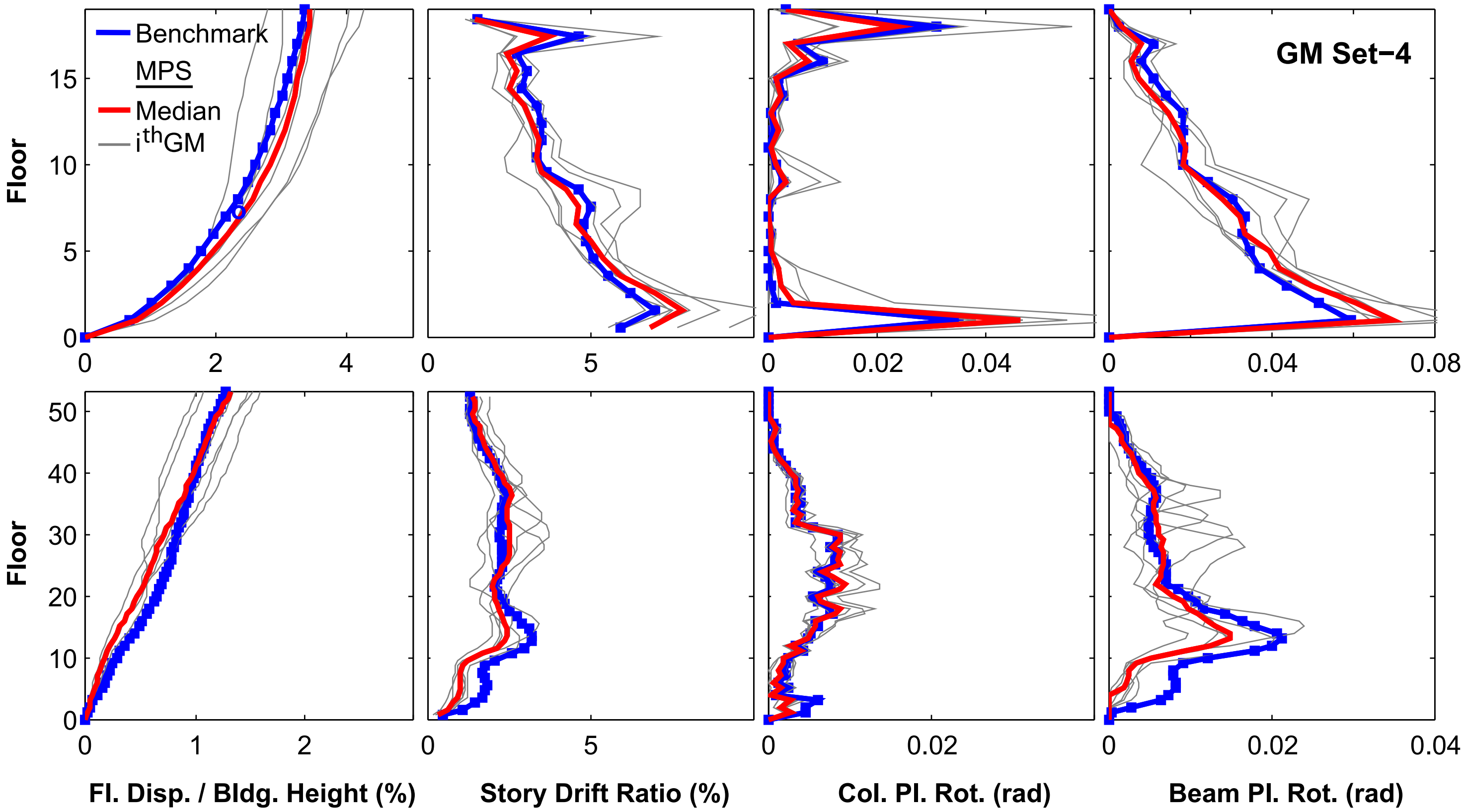

Benchmark
MPS
Median
ithGM
GM Set−4
Floor
Fl. Disp. / Bldg. Height (%)
Story Drift Ratio (%)
Col. Pl. Rot. (rad)
Beam Pl. Rot. (rad)

Figure - 13

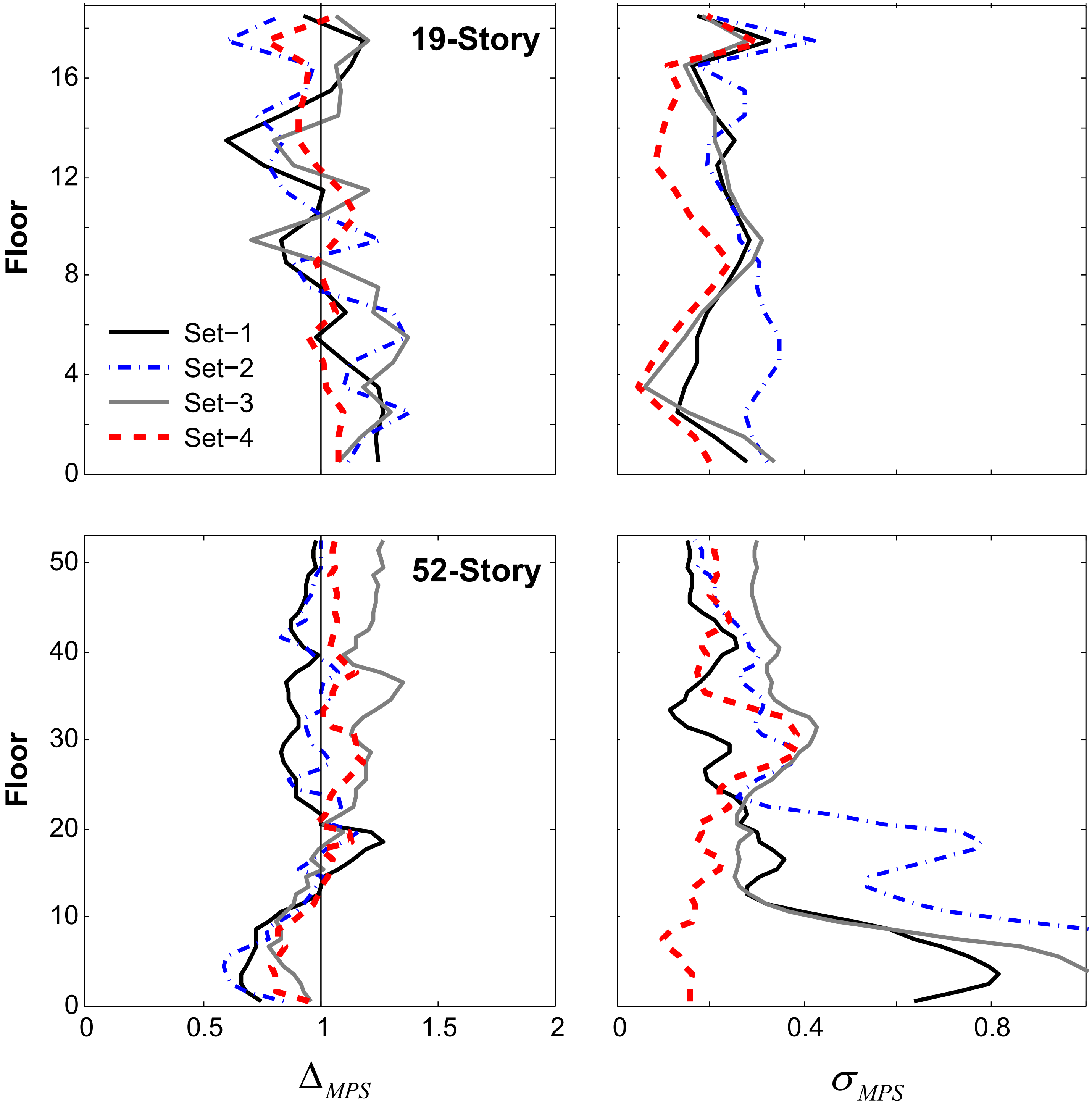

19-Story
52-Story
Floor
Floor
Set−1
Set−2
Set−3
Set−4
0
4
8
12
16
0
10
20
30
40
50
0
0.5
1
1.5
2
0
0.4
0.8
Δ_{MPS}
σ_{MPS}

Figure - 14

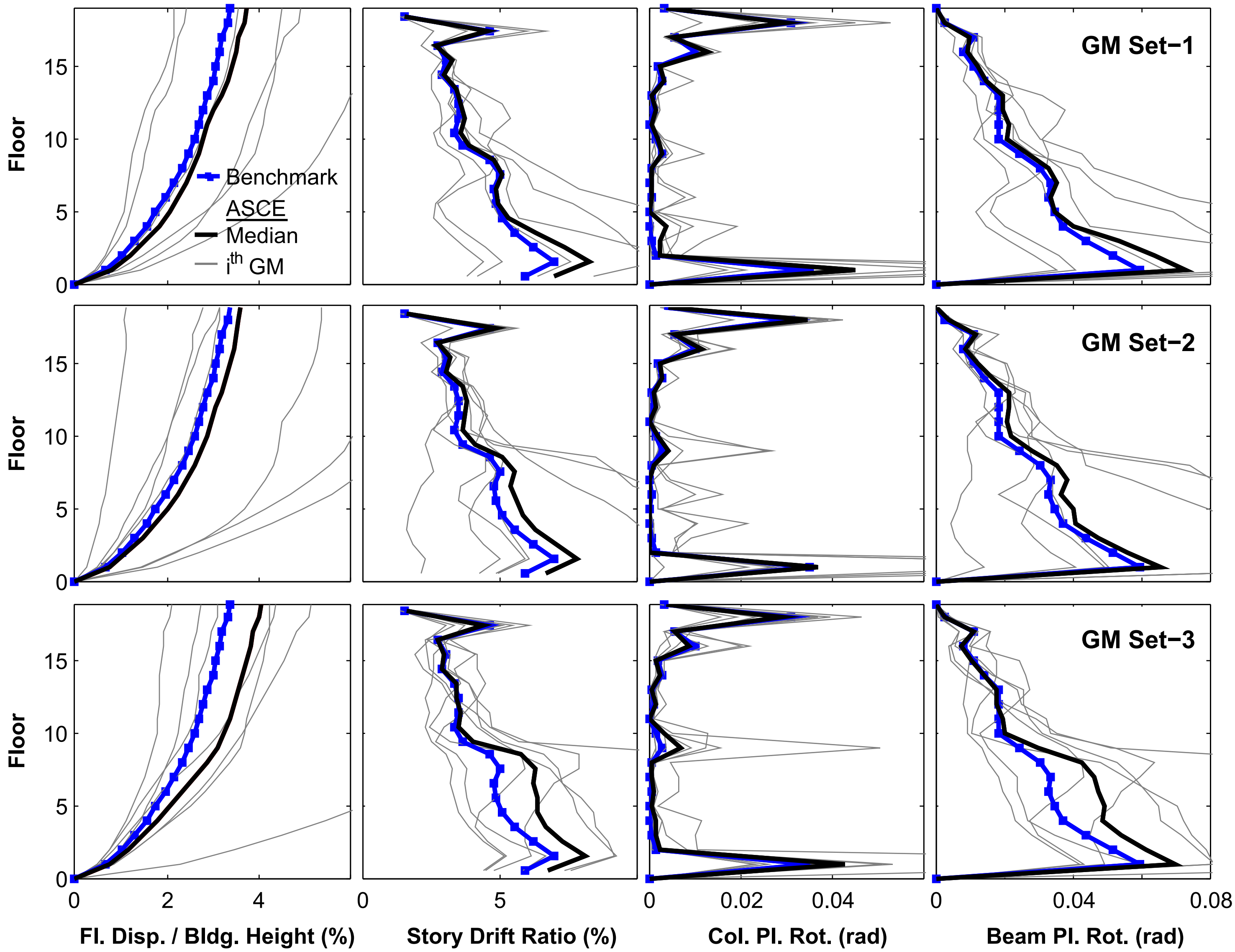
GM Set−1
GM Set−2
GM Set−3
Floor
Benchmark
ASCE
Median
i^th GM
0
5
10
15
0
2
4
0
5
0
0.02
0.04
0
0.04
0.08
Fl. Disp. / Bldg. Height (%)
Story Drift Ratio (%)
Col. Pl. Rot. (rad)
Beam Pl. Rot. (rad)

Figure - 15

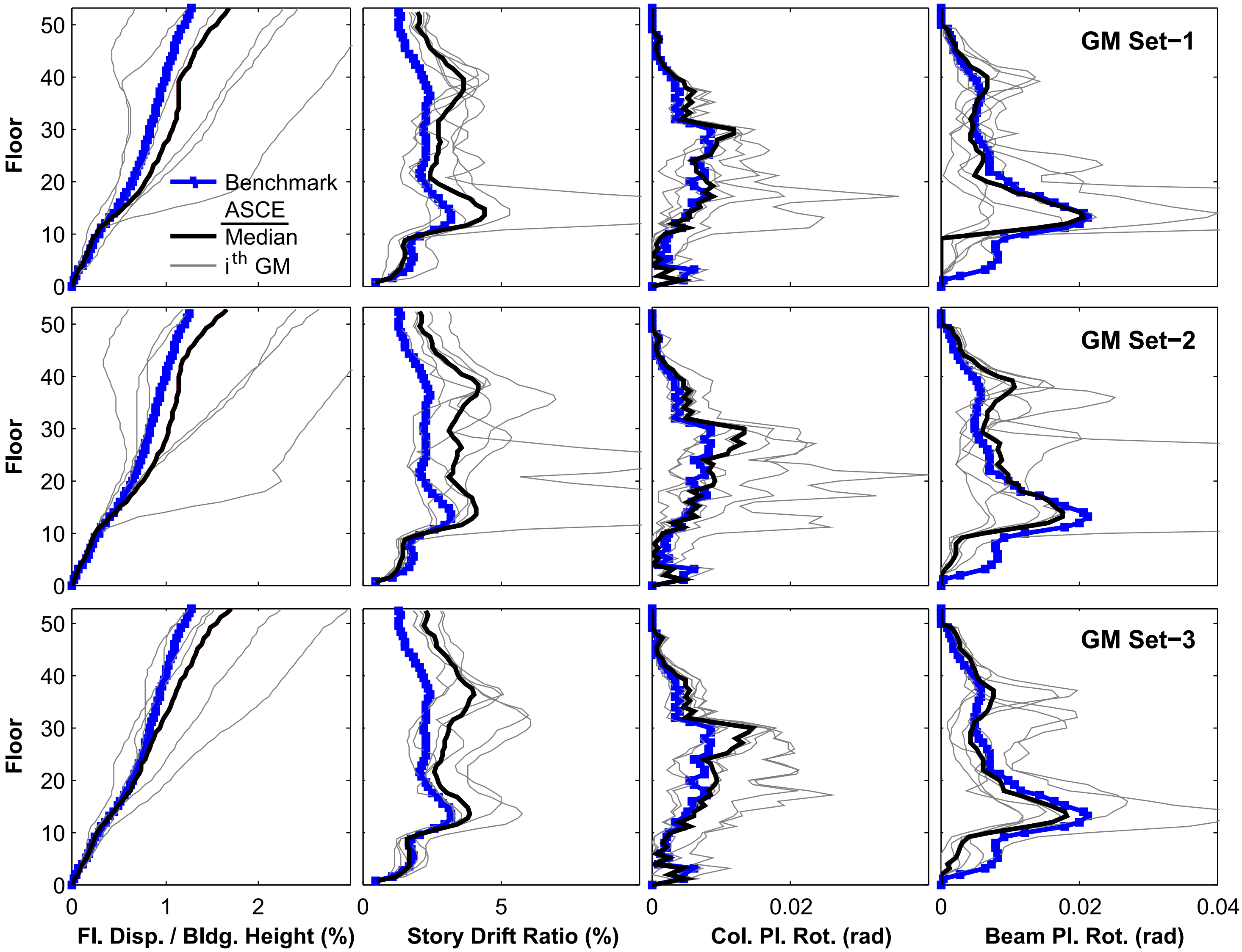

Floor
Benchmark
ASCE
Median
i th GM
GM Set−1
GM Set−2
GM Set−3
Fl. Disp. / Bldg. Height (%)
Story Drift Ratio (%)
Col. Pl. Rot. (rad)
Beam Pl. Rot. (rad)

Figure - 16

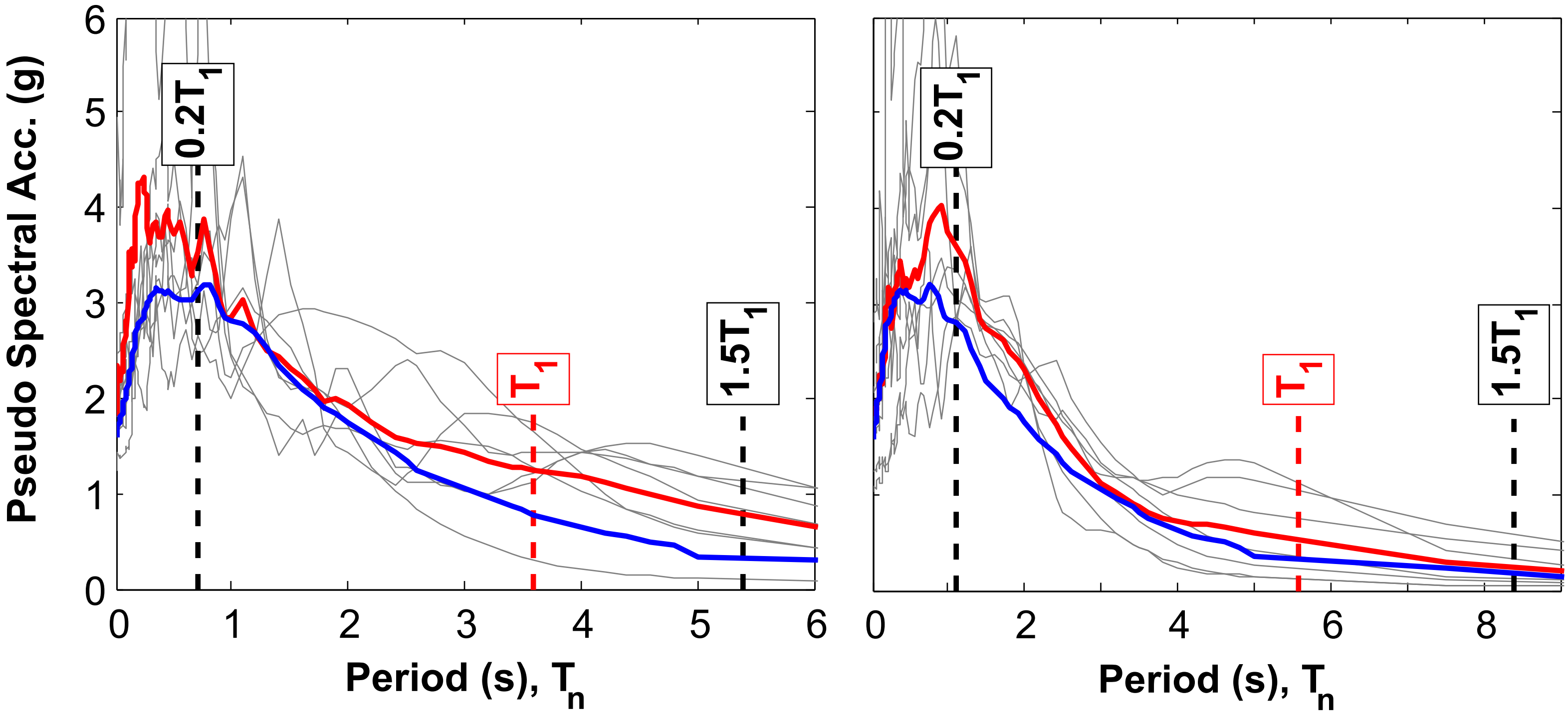

Pseudo Spectral Acc. (g)
0.2T1
T1
1.5T1
Period (s), Tn
0.2T1
T1
1.5T1
Period (s), Tn

Figure - 17

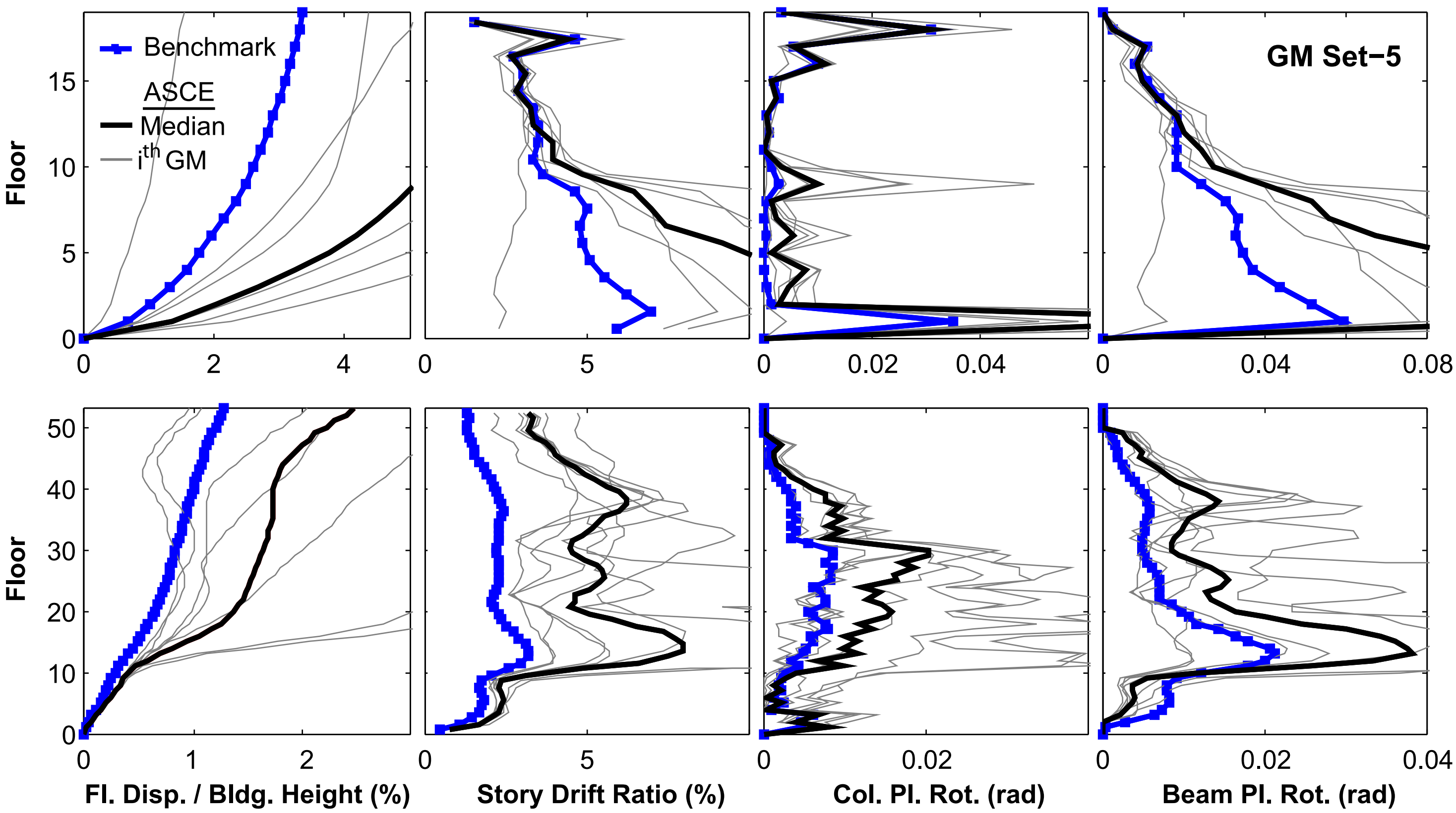

Benchmark
ASCE
Median
i^th GM
GM Set−5
Floor
15
10
5
0
0
2
4
0
5
0
0.02
0.04
0
0.04
0.08
Floor
50
40
30
20
10
0
0
1
2
0
5
0
0.02
0
0.02
0.04
Fl. Disp. / Bldg. Height (%)
Story Drift Ratio (%)
Col. Pl. Rot. (rad)
Beam Pl. Rot. (rad)

Figure - 18

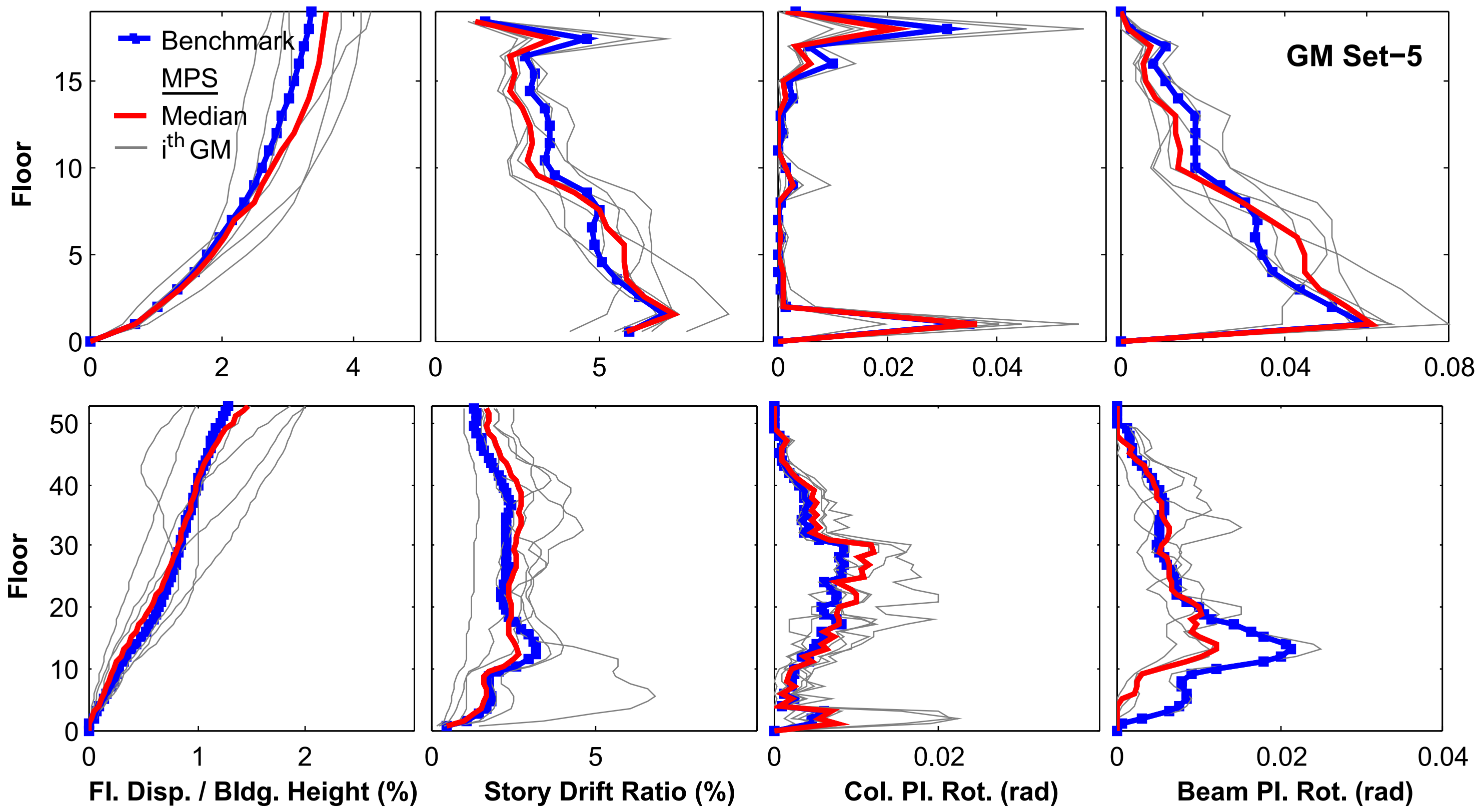

Benchmark
MPS
Median
i^th GM
GM Set−5
Floor
Fl. Disp. / Bldg. Height (%)
Story Drift Ratio (%)
Col. Pl. Rot. (rad)
Beam Pl. Rot. (rad)

Figure - 19

No.	Earthquake	Year	Station	M	R_{cl} (km)	V_{S30} (m/s)	PGA (g)	PGV (cm/s)	PGD (cm)
1	Tabas, Iran	1978	Tabas	7.4	2.1	767	0.85	110.3	61.1
2	Imperial Valley	1979	EC Meloland Overpass FF	6.5	0.1	186	0.31	79.3	28.1
3	Imperial Valley	1979	El Centro Array #7	6.5	0.6	211	0.42	80.2	41.0
4	Superstition Hills	1987	Parachute Test Site	6.5	1.0	349	0.46	74.8	36.3
5	Loma Prieta	1989	LGPC	6.9	3.9	478	0.78	77.2	42.7
6	Erzincan, Turkey	1992	Erzincan	6.7	4.4	275	0.49	72.9	24.8
7	Northridge	1994	Jensen Filter Plant	6.7	5.4	373	0.75	77.8	31.9
8	Northridge	1994	Newhall - W Pico Canyon Rd	6.7	5.5	286	0.39	76.6	43.1
9	Northridge	1994	Rinaldi Receiving Sta	6.7	6.5	282	0.63	109.2	28.3
10	Northridge	1994	Sylmar - Converter Sta	6.7	5.4	251	0.75	109.4	45.8
11	Northridge	1994	Sylmar - Converter Sta East	6.7	5.2	371	0.68	87.3	31.7
12	Northridge	1994	Sylmar - Olive View Med FF	6.7	5.3	441	0.71	97.4	22.4
13	Kobe, Japan	1995	Port Island	6.9	3.3	198	0.26	62.3	29.6
14	Kobe, Japan	1995	Takatori	6.9	1.5	256	0.65	118.8	33.4
15	Kocaeli, Turkey	1999	Yarimca	7.4	4.8	297	0.31	60.5	54.7
16	Chi-Chi, Taiwan	1999	TCU052	7.6	0.7	579	0.35	131.9	183.2
17	Chi-Chi, Taiwan	1999	TCU065	7.6	0.6	306	0.68	99.5	81.8
18	Chi-Chi, Taiwan	1999	TCU068	7.6	0.3	487	0.54	206.1	336.3
19	Chi-Chi, Taiwan	1999	TCU084	7.6	11.2	553	0.79	92.7	28.8
20	Chi-Chi, Taiwan	1999	TCU102	7.6	1.5	714	0.24	93.9	65.7
21	Duzce, Turkey	1999	Duzce	7.2	6.6	276	0.42	71.0	46.3

Table - 1

	Mode	Direction	Period (s)	
			Northridge	OpenSees
19-story Bldg.	1	E-W	3.7	3.7
	2	N-S + Torsion	3.4	3.4
	3	E-W	1.4	1.4
	4	N-S + Torsion	1.1	1.1
	5	N-S + Torsion	0.8	0.8
	6	E-W	0.6	0.6

	Mode	Direction	Period (s)		
			Northridge	Chino-Hills	OpenSees
52-story Bldg.	1	E-W	5.9	5.6	5.8
	2	Torsion	4.7	-	5.5
	3	N-S	5.6	5.3	5.4
	4	E-W	1.8	1.7	1.9
	5	Torsion	1.7	1.7	1.8
	6	N-S	1.7	1.7	1.7
	7	E-W	0.9	0.9	1.1
	8	Torsion	0.9	0.9	1.0
	9	N-S	0.9	0.9	0.9

Table - 2

				Scale Factor	
No.	**Earthquake**	**Station**	**Set**	**19-story**	**52-story**
1	Superstition Hills	Parachute Test Site	1	4.76	3.36
2	Northridge	Jensen Filter Plant	1	4.26	8.27
3	Northridge	Sylmar - Converter Sta East	1	3.86	4.41
4	Kobe, Japan	Takatori	1	6.57	5.42
5	Chi-Chi, Taiwan	TCU065	1	1.98	1.16
6	Chi-Chi, Taiwan	TCU102	1	3.28	1.99
7	Kocaeli, Turkey	Yarimca	1	3.51	3.40
1	Erzincan, Turkey	Erzincan	2	6.55	7.28
2	Imperial Valley	EC Meloland Overpass FF	2	3.46	5.01
3	Kobe, Japan	Port Island	2	2.71	4.90
4	Northridge	Sylmar - Converter Sta	2	3.03	3.06
5	Tabas, Iran	Tabas	2	2.38	1.09
6	Chi-Chi, Taiwan	TCU052	2	1.53	0.82
7	Chi-Chi, Taiwan	TCU084	2	4.53	6.11
1	Duzce, Turkey	Duzce	3	3.04	3.59
2	Imperial Valley	El Centro Array #7	3	3.08	3.39
3	Loma Prieta	LGPC	3	4.60	4.34
4	Northridge	Rinaldi Receiving Sta	3	3.43	5.39
5	Northridge	Sylmar - Olive View Med FF	3	4.43	4.80
6	Chi-Chi, Taiwan	TCU068	3	1.19	0.54
7	Northridge	Newhall - W Pico Canyon Rd	3	3.26	3.58

Table - 3

			Scale Factor
No.	Earthquake	Station	19-story
1	Superstition Hills	Parachute Test Site	4.76
2	Duzce, Turkey	Duzce	3.04
3	Erzincan, Turkey	Erzincan	6.55
4	Loma Prieta	LGPC	4.60
5	Northridge	Sylmar - Converter Sta	3.03
6	Chi-Chi, Taiwan	TCU102	3.28
7	Northridge	Newhall - W Pico Canyon Rd	3.36
			52-story
1	Superstition Hills	Parachute Test Site	3.36
2	Duzce, Turkey	Duzce	3.59
3	Imperial Valley	El Centro Array #7	3.39
4	Imperial Valley	EC Meloland Overpass FF	5.01
5	Northridge	Sylmar - Converter Sta	3.06
6	Northridge	Newhall - W Pico Canyon Rd	3.58
7	Kocaeli, Turkey	Yarimca	3.40

Table - 4